The Plant Cell, Vol. 19: 3127–3145, October 2007, www.plantcell.org © 2007 American Society of Plant Biologists

Subcellular Localization and Functional Domain Studies of DEFECTIVE KERNEL1 in Maize and *Arabidopsis* Suggest a Model for Aleurone Cell Fate Specification Involving CRINKLY4 and SUPERNUMERARY ALEURONE LAYER1 [W]

Qing Tian,[a,1,2] Lene Olsen,[b,1] Beimeng Sun,[a] Stein Erik Lid,[b] Roy C. Brown,[c] Betty E. Lemmon,[c] Kjetil Fosnes,[b] Darren (Fred) Gruis,[a] Hilde-Gunn Opsahl-Sorteberg,[b] Marisa S. Otegui,[d] and Odd-Arne Olsen[a,3,4]

[a] Pioneer Hi-Bred International, A DuPont Business, Johnston, Iowa 50131
[b] Norwegian University of Life Sciences, 1432 Ås, Norway
[c] University of Louisiana at Lafayette, Lafayette, Louisiana 70504-2451
[d] Department of Botany, University of Wisconsin, Madison, Wisconsin 53706

DEFECTIVE KERNEL1 (DEK1), which consists of a membrane-spanning region (DEK1-MEM) and a calpain-like Cys proteinase region (DEK1-CALP), is essential for aleurone cell formation at the surface of maize (*Zea mays*) endosperm. Immunolocalization and FM4-64 dye incubation experiments showed that DEK1 and CRINKLY4 (CR4), a receptor kinase implicated in aleurone cell fate specification, colocalized to plasma membrane and endosomes. SUPERNUMERARY ALEURONE LAYER1 (SAL1), a negative regulator of aleurone cell fate encoding a class E vacuolar sorting protein, colocalized with DEK1 and CR4 in endosomes. Immunogold localization, dual-axis electron tomography, and diffusion of fluorescent dye tracers showed that young aleurone cells established symplastic subdomains through plasmodesmata of larger dimensions than those connecting starchy endosperm cells and that CR4 preferentially associated with plasmodesmata between aleurone cells. Genetic complementation experiments showed that DEK1-CALP failed to restore wild-type phenotypes in maize and *Arabidopsis thaliana dek1* mutants, and DEK1-MEM also failed to restore wild-type phenotypes in *Arabidopsis dek1-1* mutants. Instead, ectopic expression of DEK1-MEM under the control of the cauliflower mosaic virus *35S* promoter gave a dominant negative phenotype. These data suggest a model for aleurone cell fate specification in which DEK1 perceives and/or transmits a positional signal, CR4 promotes the lateral movement of aleurone signaling molecules between aleurone cells, and SAL1 maintains the proper plasma membrane concentration of DEK1 and CR4 proteins via endosome-mediated recycling/degradation.

INTRODUCTION

The plant epidermis consists of specialized cell types that perform important functions such as mechanical protection, restriction of transpiration, and water and gas exchange and absorption. In addition, recent data have demonstrated that cell signaling from the epidermis plays a role in directing the growth of the inner cells in the shoot (Savaldi-Goldstein et al., 2007). In *Arabidopsis thaliana*, epidermal cells are first specified in the embryo proper as a single layer of protoderm cells on the surface of the globular embryo (Laux et al., 2004). Marker genes that are specifically expressed in the first protoderm cells, including *ARABIDOPSIS THALIANA MERISTEM LAYER1* (*ATML1*), are known, and elements in the *ATML1* promoter that are essential for its transcriptional activation have been identified (Takada and Jürgens, 2007). However, the factors driving this pattern of expression remain unknown. Later in development, the embryo protoderm gives rise to the meristematic L1 layer, and signaling by *CLV3* from this cell layer to the underlying cell layers plays a vital role in meristem function. The molecular mechanism for L1 cell layer specification and maintenance is also unknown. Extensive evidence supports the hypothesis that cell fate specification and maintenance of a monolayer of epidermal cells in plants occurs via positional signaling involving constant communication between cells (Stewart and Dermen, 1975; Kidner et al., 2000).

This conclusion was recently supported in a novel in vitro organ culture system for maize (*Zea mays*) endosperm, in which aleurone cells, the epidermal cells of the endosperm, form a monolayer on all external endosperm surfaces (Gruis et al., 2006). *Defective Kernel1* (*Dek1*) is an essential gene for this position-dependant aleurone cell formation (Becraft and Asuncion-Crabb, 2000; Gruis et al., 2006). DEK1 possesses several characteristics that are compatible with a role in cell-to-cell communication in epidermal cell fate specification. First, a predicted

[1] These authors contributed equally to this work.
[2] Current address: Monsanto Company, 800 North Lindbergh Boulevard, Creve Coeur, MO 63167.
[3] Current address: Monsanto Company, 700 Chesterfield Parkway West, Chesterfield, MO 63017.
[4] Address correspondence to odd-arne.olsen@monsanto.com.
The authors responsible for distribution of materials integral to the findings presented in this article in accordance with the policy described in the Instructions for Authors (www.plantcell.org) are: Darren (Fred) Gruis (fred.gruis@pioneer.com) for maize-related material and Hilde-Gunn Opsahl-Sorteberg (hildop@umb.no) for *Arabidopsis*-related material.
[W] Online version contains Web-only data.
www.plantcell.org/cgi/doi/10.1105/tpc.106.048868

membrane-targeting signal suggests that DEK1 is located in the plasma membrane, and second, its 21 predicted transmembrane segments with at least one potential extracytosolic loop region (DEK1-MEM; Figure 1A) suggest a role in cell-to-cell signaling (Lid et al., 2002). Although the three-dimensional structure of DEK1 is unknown, it has been speculated that the predicted extracellular portion of the molecule interacts with external ligands or membrane proteins representing positional information. Furthermore, we have proposed that external signals perceived by DEK1-MEM are transmitted via the calpain-like Cys protease (DEK1-CALP) predicted to be in the cytosol (Figure 1A) (Wang et al., 2003). Third, DEK1 is ubiquitously expressed in the endosperm, fulfilling an important requirement for a protein involved in sensing and/or transmitting cell surface positional information (Lid et al., 2002). Mutations in At *DEK1*, the unique *Arabidopsis Dek1* homolog, lead to embryos that lack a protoderm and to a partial loss of the aleurone layer (Johnson et al., 2005; Lid et al., 2005).

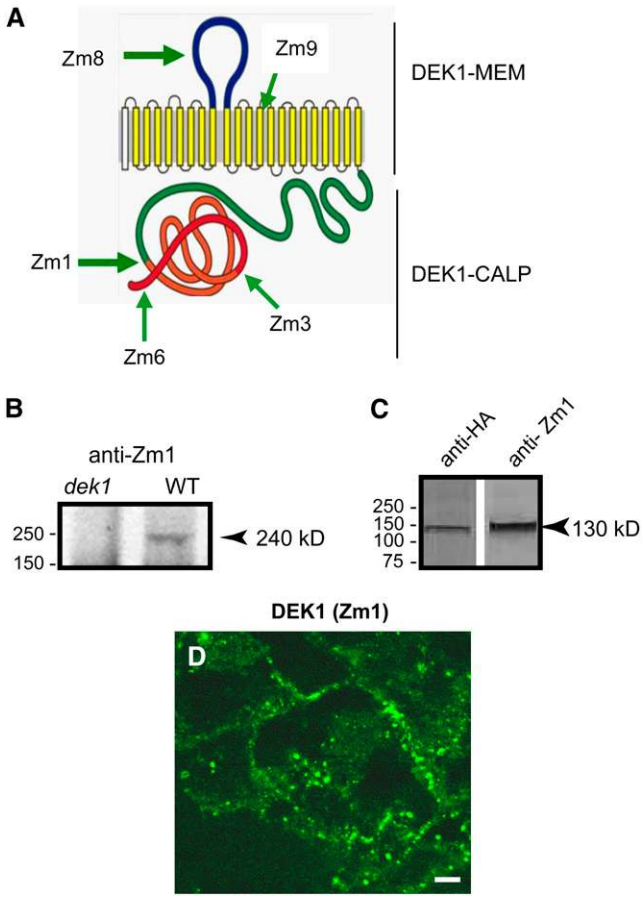

Figure 1. Zm DEK1 Antibodies and Subcellular Localization.

(A) Zm DEK1 is predicted to consist of 21 membrane-spanning segments embedded in the plasma membrane and an external loop region (DEK1-MEM). The first (unfilled) membrane-spanning segment represents a predicted signal peptide. The cytoplasmic portion harbors a calpain-like Cys proteinase (DEK1-CALP). Polyclonal antibodies were produced against peptides in the regions marked by Zm1, Zm3, Zm6, Zm8, and Zm9.

(B) Immunoblot of protein extracts from wild-type and *dek1*/*dek1* kernels at 12 DAP probed with DEK1 Zm1 antibody. The arrowhead indicates the band with the expected size (240 kD) of the DEK1 protein.

(C) Immunoblots of protein extracts from Zm Dek1-CALP:HA:FLAG:AcGFP transgenic endosperm probed with anti-HA and DEK1 Zm1 antibodies. The arrowhead indicates a band with the expected size of the fusion protein.

(D) Immunostaining of DEK1 using DEK1 Zm1 as the primary antibody and a FITC-conjugated secondary antibody. Bar = 10 μm.

No direct observations have shown the subcellular localization of the DEK1 protein. In animals, calpains consist of a highly conserved family of cytosolic calcium-dependent Cys proteases (Goll et al., 2003). Calpains have been linked to a wide variety of functions, including early embryonic development in mice (Dutt et al., 2006), muscle development (Goll et al., 2003), neuronal growth and neurodegeneration (Saito et al., 1993), cell cycle progression (Xu and Mellgren, 2002), signal cascades triggered by integrins and growth factors (Fox and Saido, 1999), membrane protrusion (Franco et al., 2004), remodeling of the cytoskeleton and cell migration (Dourdin et al., 2001; Glading et al., 2004), and the regulation of cell death via both necrosis and apoptosis (Yu et al., 2006). Animal calpains are activated in a multistep process involving translocation to the plasma membrane, activation by Ca^{2+}, and catalytic cleavage by an intramolecular process (Zalewska et al., 2004).

In addition to DEK1, CRINKLY4 (CR4) is also implicated in aleurone cell fate specification or maintenance and epidermis differentiation. The effect of the *cr4* mutation in maize endosperm shows allele-dependent variation, ranging from relatively mild, with homozygous mutant endosperms lacking small patches of aleurone cells, to severe, with large areas of aleurone cells missing (Becraft et al., 1996). *Cr4* encodes a protein receptor–like Ser/Thr kinase with a Cys-rich region with similarity to the ligand binding domain of TNFR (for Tumor Necrosis Factor Receptor) in its extracellular domain (Becraft et al., 1996). In maize, *Cr4* is also required for normal leaf epidermis development (Becraft et al., 2001). Mutations in *Arabidopsis CRINKLY4* (*ACR4*) demonstrate a role for this protein in the regulation of cellular organization during the development of leaves, sepal margins, ovule integuments, and the endothelium (Tanaka et al., 2002; Watanabe et al., 2004; Cao et al., 2005). One study using green fluorescent protein (GFP)–tagged ACR4 localized the green fluorescent signal preferentially on the lateral and basal plasma membrane domains in the epidermis of the leaf primordia (Tanaka et al., 2002). A second study detected ACR4 in anticlinal and inner periclinal plasma membranes of epidermal cells in ovules (Gifford et al., 2003). A recent report concluded that ACR4 is internalized from the plasma membrane via a brefeldin A–sensitive pathway, being detectable in two compartments in root cells: protein export bodies and a population of internalized vesicles (Gifford et al., 2005). The authors concluded that the internalization and turnover of ACR4 are linked and depend on functionality, suggesting that ACR4 signaling may be subjected to endocytosis, endosomal trafficking, and degradation.

Although several observations appear to suggest that DEK1 and CR4 may act in the same pathway, including the enhanced severity of leaf and embryo phenotypes when weak *cr4* and *dek1*

alleles are combined in both maize and *Arabidopsis*, a firm experimental basis for this conclusion is still lacking (Johnson et al., 2005). The *Cr4* transcript was detectable in *dek1* mutant kernels, indicating that *Dek1* transcript or protein was not required for *Cr4* transcript accumulation (Becraft et al., 2002). As stated above, CR4 bears similarity to the ligand binding motif of TNFR. In animals, two TNFRs bind the tumor necrosis factor (TNF) ligand, a proinflammatory cytokine that plays an important role in diverse cellular events such as cell proliferation, differentiation, and death (Locksley et al., 2001; MacEwan, 2002; Aggarwal, 2003). Both receptors belong to the TNF/nerve growth factor receptor superfamily, all of which have multiple Cys-rich domains of the type found in CR4. However, the mechanism by which CR4 affects epidermal cell fate specification in plants is unknown.

A third protein identified in maize affecting aleurone cell development, SUPERNUMERARY ALEURONE LAYERS1 (SAL1) (Shen et al., 2003), encodes a predicted 204–amino acid protein that is a homolog of human CHMP1 (for CHARGED VESICULAR BODY PROTEIN1/CHROMATIN-MODULATING PROTEIN1) (Howard et al., 2001) and yeast DID2 (for DOA4-INDEPENDENT DEGRADATION2) (Nickerson et al., 2006), members of a conserved gene family encoding class E vacuolar sorting proteins. It is well established that integral membrane proteins are sorted into luminal vesicles of late multivesicular endosomes. These luminal vesicles and their cargos are subsequently degraded in lysosomes upon fusion of the limiting endosomal membrane with the lysosomal membrane (Babst, 2005). The sorting of transmembrane cargo proteins into the lumenal vesicles of endosomes depends on the recruitment of endosomal sorting complexes required for transport (ESCRTs) to the cytosolic face of endosomal membranes. The subsequent dissociation of ESCRTs from endosomes requires VPS4P, and DID2P coordinates the dissociation of ESCRT-III from endosomes (Nickerson et al., 2006). Mutations in *Sal1*, *sal1-1* and *sal1-2*, cause the differentiation of up to seven layers of aleurone cells in maize endosperm (Shen et al., 2003). The molecular mechanism creating this phenotype is unknown, but one possibility is that the concentration of membrane molecules regulating aleurone cell specification is controlled by degradation through the endosomal pathway and that the *sal1* mutation leads to an accumulation of such molecules at the membrane, which in turn results in an increased number of aleurone cell layers. In tobacco (*Nicotiana tabacum*), virus-induced silencing of *Sal1* resulted in only mild alteration of leaf structure and color without significantly affecting plant architecture (Yang et al., 2004).

Here, we present data to support the conclusion that DEK1-CALP alone does not restore wild-type function in complementation experiments with the maize and *Arabidopsis dek1* mutants. We also show that DEK1-MEM overexpression leads to a dominant negative phenotype. Immunolocalization experiments show that DEK1 and CR4 colocalize at the plasma membrane and in endosomes and that SAL1 colocalizes with DEK1 and CR4 in endosomes. Finally, we establish that aleurone cells of in vitro–grown endosperm form symplastic domains via enlarged plasmodesmata in periclinal walls and that *Cr4* preferentially accumulates in plasma membranes associated with these plasmodesmata.

RESULTS

DEK1 Localizes to the Plasma Membrane and to Endosomal Compartments

DEK1 is predicted to have 21 membrane-spanning domains, a loop region on the extracytosolic side, and a calpain Cys proteinase domain in the cytosol (Figure 1A). Available sequence data from angiosperms as well as gymnosperms demonstrate a remarkable degree of sequence conservation for DEK1 (Lid et al., 2002). For example, the maize and *Arabidopsis* homologs have an overall identity of 70% over the 2129 amino acids of maize DEK1, the identity being highest in the calpain domain, 86% (Lid et al., 2002). For the DEK1 homolog of the gymnosperm loblolly pine (*Pinus taeda*), the identity to maize DEK1 is 79% in the calpain domain (Lid et al., 2002). Recently, the conserved nature of DEK1 throughout plant evolution was confirmed by the DEK1 sequence of the moss *Physcomitrella patens*, separated from angiosperms by ~500 million years of evolution (Quatrano et al., 2007). Amino acid sequence comparison of DEK1 from moss and maize reveals 59% identity and a similarity of 74%. In the calpain domain, the identity is even higher, ~80%.

In order to determine the subcellular localization of DEK1, polyclonal peptide antibodies were generated in rabbits against five different regions of DEK1 (Figure 1A), all of which showed high affinity to their corresponding peptides. To validate these DEK1 antibodies, protein extracts from 12-DAP (for days after pollination) *dek1*/*dek1* and wild-type kernels were probed on immunoblots with Zm1 antibody raised against a peptide in the DEK1-CALP domain. The Zm1 antibody labeled a protein band of the expected size for DEK1 (240 kD) only in wild-type, but not in *dek1*/*dek1*, endosperm (Figure 1B). To validate the ability of the Zm1 antibody to recognize DEK1, we expressed the fusion protein ZmDEK1-CALP:HA:FLAG:AcGFP in maize under the control of the 27-kD γ-*Zein* promoter, expected to give high levels of the transcript in starchy endosperm (Ueda and Messing, 1991; Russell and Fromm, 1997). Immunoblot analysis using Zm1 antibody on extracts from 20-DAP GFP-positive endosperm recognized a protein band at the expected size for the fusion protein, the identity of which was confirmed using a commercial hemagglutinin (HA) antibody (Figure 1C). Next, we performed immunolabeling experiments to test the ability of Zm1 antibody to recognize DEK1 protein in sections from these GFP-expressing endosperms using Zm1 antibody with rhodamine-conjugated secondary antibody. The endosperm sections used in this experiment as well as in other experiments throughout this study were transverse sections of in vitro–grown endosperm in which the outer cell layer consisted of aleurone cells and the interior cells were starchy endosperm cells (Gruis et al., 2006). In this experiment, the green GFP signal and the red signal from the rhodamine-conjugated antibody overlapped, supporting the conclusion that Zm1 antibody recognized DEK1 in situ (see Supplemental Figures 1A to 1C online).

The Zm1 antibody was then used to label endogenous DEK1 in sections of wild-type endosperms harvested at 6 DAP and grown in vitro for 8 d. As shown in Figure 1D, the Zm1 antibody labeled the plasma membrane and distinct ~500-nm compartments in the cytoplasm. As a negative control for immunostaining, we

omitted the primary antibody and used only fluorescein isothiocyanate (FITC)– or rhodamine-conjugated secondary antibodies. Only faint diffused signals representing background were detected in the red and green channels (see Supplemental Figures 1D and 1E online). The same localization pattern described in Figure 1D was also observed using the antibodies against the DEK1 regions Zm8, Zm3, Zm6, and Zm9 (data not shown). As a final test of the specificity of the DEK1 antibodies in immunolocalization experiments, we used DEK1 peptide Zm8 (Figure 1A) to block the binding of the Zm8 antibody to endogenous DEK1 (see Supplemental Figures 1F and 1G online). In these experiments, staining associated with the plasma membrane as well as the ~500-nm cytoplasmic compartments was lost when incubated with the Zm8 peptide but not the control peptide, supporting the conclusion that the DEK1 antibody recognized the endogenous DEK1 protein. Motivated by the need to carry out double labeling experiments, we also developed a rat antibody against the Zm1 peptide, named Zm1-2, that labeled the same subcellular structures as the rabbit Zm1 antibody (see Supplemental Figures 1H to 1J online).

To investigate the possibility that the ~500-nm organelles labeled by DEK1 antibodies were endosomes, in vitro–grown endosperms were incubated with the endocytotic marker FM4-64. For unknown reasons, the dye was not internalized by endosperm cells. Since DEK1 showed the same localization pattern in root cells as in endosperm cells (i.e., at the plasma membrane and on the punctate cytoplasmic compartment) (Figure 2), we used maize roots for our FM4-64 experiments. Fifteen minutes after incubation of intact young maize roots in fixable FM4-64, the FM4-64 signal was observed in plasma membranes and in punctate structures in the cytoplasm that we interpreted to be endocytic compartments, likely endosomes. When fixed FM4-64–stained samples were immunolabeled with DEK1 Zm1 (Figures 2A to 2C) and Zm8 (Figures 2D to 2F) antibodies, both stained FM4-64–positive organelles, suggesting that DEK1 localizes to endosomal compartments.

DEK1-CALP Failed to Fully Complement the *dek1* Mutant Phenotypes in Maize and *Arabidopsis*

We previously proposed that DEK1 plays a role in maintaining aleurone cell identity by acting as a calpain on an unknown substrate(s) and that this activity is regulated by DEK1-MEM (Lid et al., 2002). Here, we examined whether DEK1-CALP alone is capable of functionally complementing the *dek1* mutant phenotype of maize and *Arabidopsis*. First, we crossed maize plants that expressed Zm DEK1-CALP under the control of the 27-kD γ-*Zein* promoter with heterozygous *Dek1*/*dek1* plants. After one round of self-pollination, we investigated the segregation ratio of wild-type versus *dek1*/*dek1* grains. In all crosses, we observed a 3:1 ratio of wild-type to typical *dek1* endosperms lacking aleurone cells. These experiments showed that Zm DEK1-CALP alone is incapable of rescuing the *dek1* mutant maize endosperm phenotype when expressed under the control of the 27-kD γ-*Zein* promoter.

Next, we expressed At DEK1-CALP in heterozygous *DEK1*/*dek1-1 Arabidopsis* plants under the control of the At *DEK1* promoter that we had previously used to complement the *dek1-1* mutant phenotype (Lid et al., 2005). Self-pollinated *DEK1*/*dek1-1* plants are expected to carry a ratio of 3:1 wild-type to collapsed

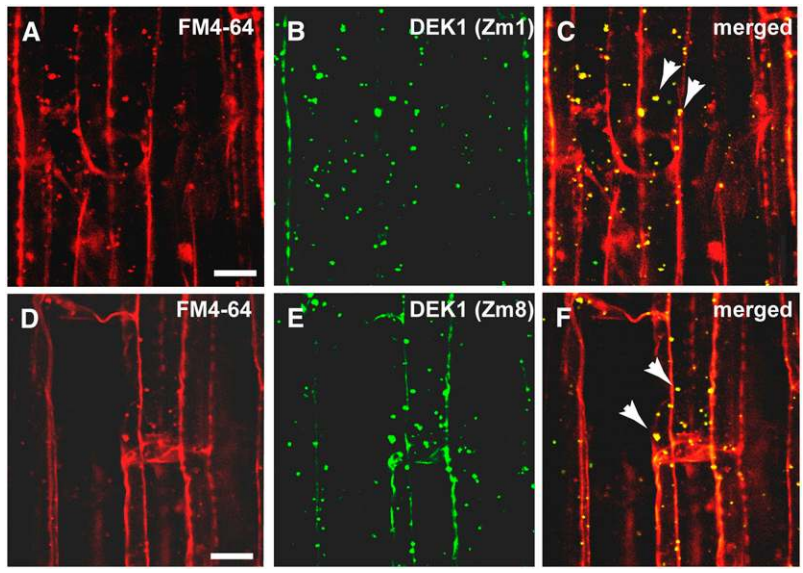

Figure 2. Colocalization of DEK1 and FM4-64 in Endocytotic Compartments.

(A) to **(C)** Confocal microscopy images of maize root cells stained with FM4-64 **(A)** and with the DEK1 Zm1 antibody and a secondary antibody conjugated with FITC **(B)**. **(C)** shows a merged image of **(A)** and **(B)**. Yellow indicates overlapping fluorescent signal (arrowheads).
(D) to **(F)** Confocal microscopy images of root cells stained with the endocytic marker FM4-64 **(D)** and DEK1 Zm8 antibody with a FITC-conjugated secondary antibody **(E)**. **(F)** shows a merged image of **(D)** and **(E)**. Yellow indicates overlapping fluorescent signal (arrowheads).
Note the colocalization between DEK1 antibodies and FM4-64 in punctate cytoplasmic structures, likely endosomes (arrowheads) Bars = 5 μm.

dek1-1 seeds (Lid et al., 2005). Instead, plants that segregated for *DEK1*/*dek1-1* as well as the transgene carried only 15% of typical collapsed *dek1-1* mutant seeds (Figure 3). Upon closer inspection, the 10% deficit of typically collapsed seeds could be accounted for by a novel class of intermediate-type defective seeds that failed to turn green but did not fully collapse when the seeds matured (Figure 3A). Microscopy examination revealed that, in contrast with typical *dek1-1* seeds with underdeveloped endosperm and embryo, the intermediate seeds developed a larger endosperm that was retained longer than normal (Figures 3B to 3D). In wild-type seeds, the whole endosperm, with the exception of the aleurone layer, became degraded as the embryo reached maturity (Figures 3B and 3E). Similar to typical *dek1-1* endosperm, the intermediate seed type failed to differentiate an aleurone layer (Figure 3F), which is clearly observable in the late developmental stages of wild-type seeds (Figure 3E). The embryos of the intermediate seeds were typically larger and contained more cells (Figure 3G) than the homozygous *dek1-1* embryos (Figure 3H). Similar to *dek1-1* knockout embryos, embryos of the intermediate seed type lacked proper organ formation. The same phenotypic ratio of seeds described above was also obtained in complementation experiments in *Arabidopsis* with Zm DEK1-CALP (overall 70% identity to At DEK1-CALP) (Lid et al., 2002) (data not shown). These results showed that although DEK1-CALP improved the growth of both endosperm and embryos of homozygous *dek1-1* seeds, a full complementation

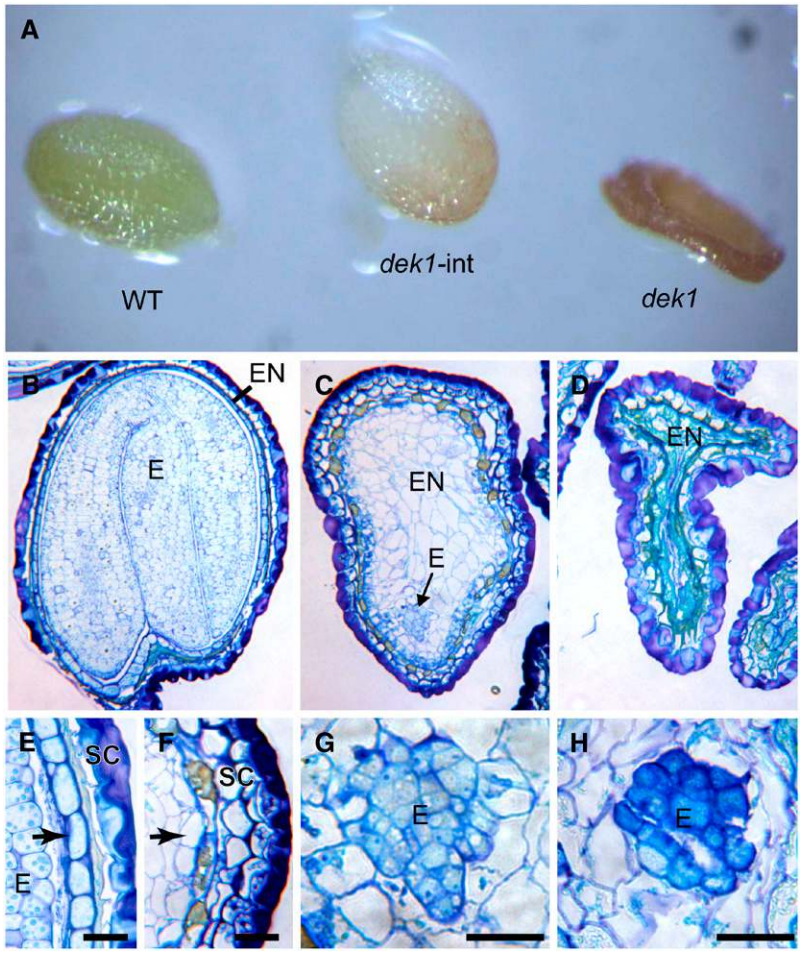

Figure 3. The DEK1 Calpain Cys Proteinase Domain Alone Is Unable to Fully Complement the *dek1* Mutant Phenotype in *Arabidopsis*.

(A) *Arabidopsis* seeds from a *DEK1*/*dek1-1* plant transformed with the At *DEK1-CALP* expression cassette under the control of the At *DEK1* promoter, showing segregation of a wild-type seed (WT), an intermediate phenotype seed (*dek1*-int), and a collapsed *dek1-1* seed (*dek1*).
(B) to **(D)** Longitudinal sections of *Arabidopsis* seed types shown in **(A)**: wild-type seed **(B)**; intermediate seed type **(C)**; and typical collapsed *dek1-1* seed **(D)**.
(E) Detail from a wild-type seed with a peripheral aleurone layer (arrow).
(F) Detail from an intermediate seed type lacking aleurone differentiation in the peripheral position of the endosperm (arrow).
(G) An embryo from intermediate type seeds.
(H) A typical *dek1-1* embryo.
E, embryo; EN, endosperm; SC, seed coat. Bars = 50 μm.

of the aleurone and embryo phenotypes to the wild type did not occur.

Plants with Ectopic Expression of At DEK1-MEM in *Arabidopsis* Have Similar Phenotypes as At *DEK1* RNA Interference Plants

DEK1-MEM has been proposed to regulate the DEK1 calpain Cys proteinase activity (Lid et al., 2002). To further investigate the role of the DEK1-MEM domain, we expressed At DEK1-MEM in wild-type *Arabidopsis* plants under the control of the At *DEK1* and cauliflower mosaic virus (*CaMV*) *35S* promoters. In these experiments, we expressed both untagged At DEK1-MEM protein and an At DEK1-MEM-GFP fusion protein, with both constructs giving identical phenotypes.

Whereas the expression of At DEK1-MEM and At DEK1-MEM-GFP in wild-type plants under the control of the At *Dek1* promoter caused no deviating phenotype from the wild type, the overexpression of the At DEK1-MEM and At DEK1-MEM-GFP proteins with the *CaMV35S* promoter resulted in a gradient of developmental aberrations, ranging from plants with defective shoot apical meristems unable to produce adult leaves (Figures 4A and 4B) to cotyledons with lack of or disorganized epidermal cells (Figures 4C and 4D) to plants producing radialized rosette leaves (Figure 4E). To demonstrate that the overexpressed At DEK1-MEM proteins were targeted to plasma membranes, we performed immunolabeling in roots overexpressing At DEK1-MEM-GFP with an anti-GFP antibody. These experiments confirmed the presence of the fusion protein in the plasma membrane of root cells (see Supplemental Figure 2A online).

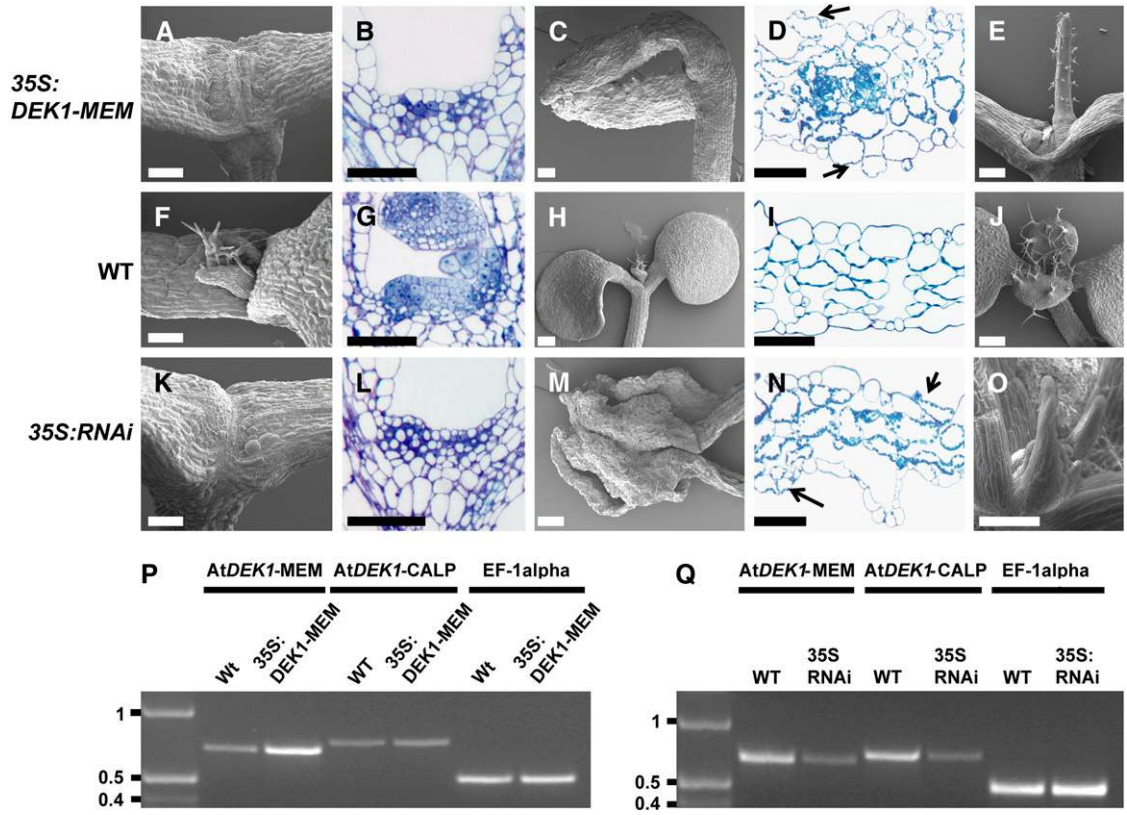

Figure 4. Phenotypic Analysis of *Arabidopsis* Lines Expressing At *DEK1-MEM* and At *DEK1*-RNAi.

(A) to **(E)** Phenotypes of At *DEK1-MEM* seedlings.
(F) to **(J)** Comparable developmental stages and organs in wild-type seedlings.
(K) to **(O)** Comparable developmental stages and organs in At *DEK1*-RNAi seedlings.
The shoot apex is severely affected in At *DEK1-MEM* plants (**[A]** and **[B]**) and severely affected in RNAi lines (**[K]** and **[L]**). Cotyledons from At *DEK1-MEM* **(C)** and At *DEK1*-RNAi **(M)** seedlings are also distorted. Note in the cross sections of cotyledons from At *DEK1-MEM* **(D)** and At *DEK1*-RNAi **(N)** plants that the cells exposed to both adaxial and abaxial surfaces contain chloroplasts, suggesting that they have not completely differentiated into epidermal cells. Shoot apices from less severely affected seedlings in both At *DEK1-MEM* and At *DEK1*-RNAi lines can display one terminal radialized rosette leaf **(E)** or several radial rosette leaves **(O)**. Bars = 100 μm.
(P) and **(Q)** RT-PCR analyses showing At *DEK1* transcripts in At *DEK1-MEM* and wild-type seedlings **(P)** and in At *DEK1*-RNAi and wild-type seedlings **(Q)**. The three primer sets used, specific for the At *DEK1-MEM* region, the At *DEK1*-CALP region, and EF-1α as a control to monitor template presence, are indicated at top. DNA marker sizes are indicated at left in kb.

In order to provide a baseline for At *DEK1*-MEM overexpression phenotypes, we also expressed an At *DEK1* RNA interference (RNAi) construct under the control of the *CaMV35S* promoter to generate *DEK1* knockout phenotypes. Phenotypes shown here for the At *DEK1*-RNAi construct were comparable to those observed previously (Johnson et al., 2005) in a similar experiment. For a comparison with the At *DEK1*-MEM–overexpressing plants, wild-type phenotypes are shown in Figures 4F to 4J.

Interestingly, the phenotypes of the At *DEK1*-MEM–overexpressing plants very closely mimicked the range of phenotypes observed in plants expressing the At *DEK1*-RNAi construct (Figures 4K to 4O), suggesting that overexpression of the DEK1 membrane anchor domain induces a dominant negative effect comparable to the loss or downregulation of DEK1 function. Structural alterations were observed in ~50% of the obtained independent T1 lines expressing the At *DEK1*-MEM and At *DEK1*-RNAi constructs. The most severe phenotypes observed when overexpressing At *DEK1*-MEM (Figure 4A) and At *DEK1*-RNAi (Figure 4K) included seedlings grown on agar that did not produce rosette leaves and died within 2 weeks after being transferred to soil. Microscopy analysis of the shoot apex showed that in contrast with the wild type, consisting of densely cytoplasmic cells organized into the L1 to L3 cell layers (Figure 4G), the meristems of the At *DEK1*-MEM–expressing (Figure 4B) and At *DEK1*-RNAi–expressing (Figure 4L) plants contained vacuolated cells lacking a layered meristem organization. The At *DEK1*-MEM– and At *DEK1*-RNAi–expressing plants (Figures 4C and 4M, respectively) that did not produce rosette leaves also displayed a disorganized cell organization on the cotyledon surfaces. On these cotyledons, the epidermal cell identity appeared partially lost, as shown by the appearance of chloroplast-containing cells on the cotyledon surfaces (Figures 4D and 4N), in contrast with the wild type, in which chloroplasts were only present in internal mesophyll cells (Figure 4I).

The largest and less severely affected class of both At *DEK1*-MEM– and At *DEK1*-RNAi–expressing plants displayed radialized rosette leaves. This phenotype was manifested either as one terminal organ with no further organ development from the shoot apex, as exemplified in the At *DEK1*-MEM plants shown in Figure 4E, or, more frequently, as a series of two to five radialized leaves emanating from the shoot apex, as exemplified in the At *DEK1*-RNAi–expressing plants shown in Figure 4O. In the latter case, the shoot apical meristems appeared normal and subsequent rosette leaves beyond the first few radialized leaves developed normally (data not shown). Although the radialized leaves initially lacked trichomes, they invariably developed trichomes evenly distributed around the circumference of the leaves as leaf growth continued. Thus, as trichomes are normally restricted to the adaxial leaf surface in wild-type plants, we infer that the radialized leaves observed in the At *DEK1*-MEM– and At *DEK1*-RNAi–expressing plants were adaxialized.

Additional experiments were performed to elucidate the nature of the observed phenotypes. In order to rule out the possibility that the DEK1-MEM phenotype represents a pleiotropic effect caused by ectopic expression of a large membrane protein, we expressed a version of At DEK1-MEM that lacked the loop region (DEK1-MEM-DEL) (Figure 1A). In total, we studied 51 plants with FLAG-tagged (at both the 5′ and 3′ ends) and His-tagged DEK1-MEM-DEL, all of which were indistinguishable from wild-type control plants. In addition, the presence of DEK1-MEM-DEL-FLAG in the plasma membrane was demonstrated by immunolabeling (see Supplemental Figure 2B online). These results support the conclusion that the phenotypes are caused specifically by the overexpression of DEK1-MEM. RT-PCR analyses showed that plants transformed with the *CaM35S*:At *DEK1-MEM* construct had a higher level of At *DEK1-MEM* transcript than the wild-type control. *DEK1*-RNAi plants showed lower At *DEK1* transcript levels than wild-type control plants (Figures 4P and 4Q). This indicates that the phenotypes observed were not caused by silencing of the native At *DEK1* gene.

CR4 Is Also Localized to the Plasma Membrane and Endosomes in Maize

Antibodies were raised against the maize CR4 external and cytosolic domains, GR2 and GR8, respectively (Figure 5A). Using these antibodies in immunoblot analysis with extracts from *cr4*/*cr4* and wild-type plants, we detected a protein band with the expected size of CR4 (~95 kD) in wild-type, but not in *cr4*/*cr4*,

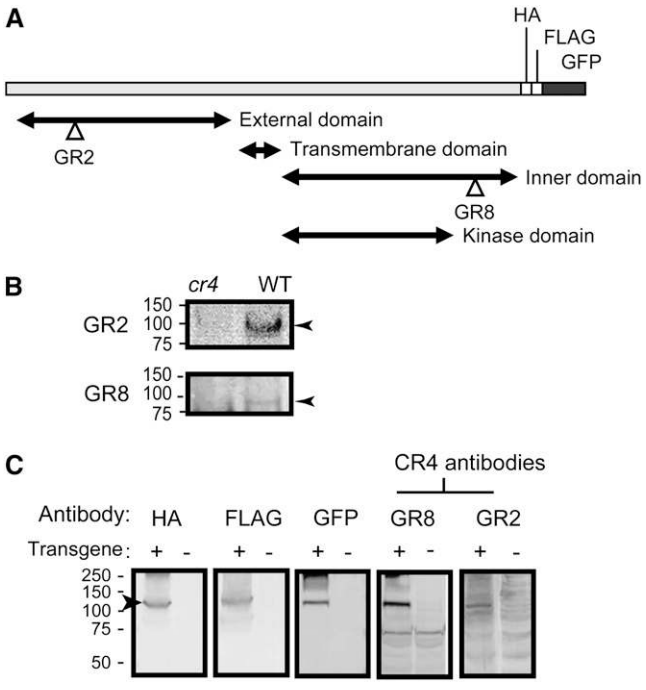

Figure 5. CR4 Antibodies Recognize Zm CR4 in Wild-Type and Transgenic Maize Seeds.

(A) Domain structure and location of peptides used to generate Zm CR4 antibodies.

(B) Immunoblots of protein extracts from wild-type and *cr4* mutant maize roots probed with CR4 GR2 and GR8 antibodies. Arrowheads indicate the band with the expected size of the CR4 protein (~95 kD).

(C) Immunoblots using protein extracts from CR4:HA:FLAG:AcGFP transgenic endosperms (+) or nontransgenic endosperm controls (−) probed with GFP and CR4 antibodies. The arrowhead indicates the fusion protein at 127 kD.

samples (Figure 5B). To further characterize these antibodies, we expressed the construct CR4:HA:FLAG:AcGFP under the control of the 27-kD γ-*Zein* promoter in maize (Figure 5C). Transgenic 10-DAP endosperm expressed GFP in T2 kernels from nine independent transformation events. The GFP signal intensified up to 30 DAP, consistent with the known temporal activity of the 27-kD γ-*Zein* promoter (Ueda and Messing, 1991; Russell and Fromm, 1997). Immunoblot analysis of extracts from these transgenic endosperms detected the expected 127-kD CR4:HA:FLAG:AcGFP fusion protein using antibodies against epitope tags as well as the CR4 peptide antibodies GR2 and GR8 (Figure 5C).

We then studied the subcellular localization of CR4 in transgenic in vitro–grown endosperms using GFP fluorescence from the CR4:HA:FLAG:AcGFP fusion protein. In these endosperms, the GFP signal was detectable in the plasma membrane and in small spherical cytoplasmic compartments (Figure 6A). To corroborate these observations, we also immunolabeled the endosperms expressing GFP-tagged CR4 with GR2 antibody, observing a high degree of colocalization of the two signals to the punctate structure on the plasma membrane (see Supplemental Figures 3A to 3C online). We then labeled CR4-GFP–positive endosperms with DEK1 antibody and showed that CR4 and DEK1 colocalized at the plasma membrane as well as in punctate structures in the cytosol (Figures 6B and 6C). The subcellular localization pattern for CR4 was similar in root tissues and in endosperm cells (Figures 6A and 6D). Finally, root samples previously incubated in the endocytic dye FM4-64 were immunolabeled with CR4 antibody and a FITC-conjugated secondary antibody. This experiment showed colocalization between the FM4-64 signal and CR4 staining (Figures 6D to 6F), suggesting that the cytosolic CR4-positive organelles are endocytic compartments, likely endosomes. From these experiments, we concluded that CR4 colocalizes with DEK1 at the plasma membrane and in endosomes.

CR4 Concentrated in Plasma Membrane Domains Associate with Plasmodesmata That Connect Aleurone Cells

To further characterize the subcellular localization of CR4 in maize in vitro–grown endosperm, we performed immunogold labeling on high-pressure frozen/freeze-substituted material (Figure 7). Using CR4 GR2 antibody, we confirmed that CR4 localized to plasma membranes of both aleurone and starchy endosperm cells (Figures 7A to 7F). Interestingly, the highest density of CR4 labeling was found at plasma membrane domains of plasmodesmata located at the anticlinal cell walls between aleurone cells (Figures 7B to 7D). Whereas 1.8 ± 1.03 gold particles per 500 nm of plasma membrane in cross section were observed at the plasmodesmata between aleurone cells, only 0.3 ± 0.23 gold particles per 500 nm of plasma membrane in cross sections were recorded elsewhere in the aleurone cells. This means that CR4 is approximately six times more abundant at aleurone plasmodesmata than in any other plasma membrane domain. By contrast, the CR4 labeling on plasmodesmata between starchy endosperm cells was low and did not drastically differ from the labeling of the remaining plasma membrane domains in the starchy endosperm cells (Figure 7F).

The observation that CR4 is associated with plasmodesmata prompted us to look closer at the distribution and structure of plasmodesmata in in planta– and in vitro–cultivated endosperms. We obtained dual-axis electron tomograms of high-pressure frozen/freeze-substituted aleurone and starchy endosperm cells, and by imaging the reconstructed volume in different X, Y, and Z settings, we were able to determine the precise size, shape, and

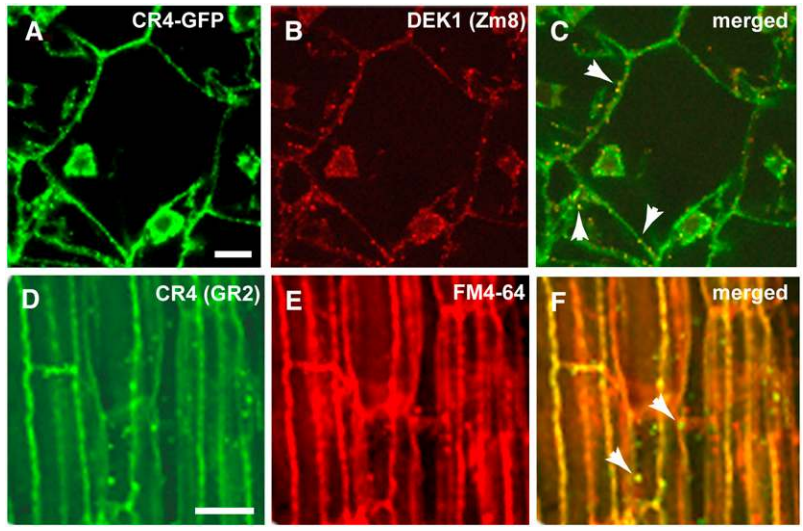

Figure 6. Colocalization of CR4 and DEK1 in Endosomes.

(A) to **(C)** Colocalization of CR4 **(A)** and DEK1 **(B)** in in vitro–grown CR4:HA:FLAG:AcGFP transgenic maize endosperm. **(C)** shows a merged image of **(A)** and **(B)**. The GFP signal and the DEK1 signal overlapped on plasma membrane and punctate structures in the cytoplasm (arrowheads). Bar = 20 μm. **(D)** to **(F)** Wild-type maize root sections immunostained with GR2 antibody and a secondary antibody conjugated with FITC **(D)**. **(E)** shows staining with FM-4-64. **(F)** shows the two signals colocalized on plasma membrane and in punctate structures in the cytoplasm, likely endosomes (arrowheads). Bar = 10 μm.

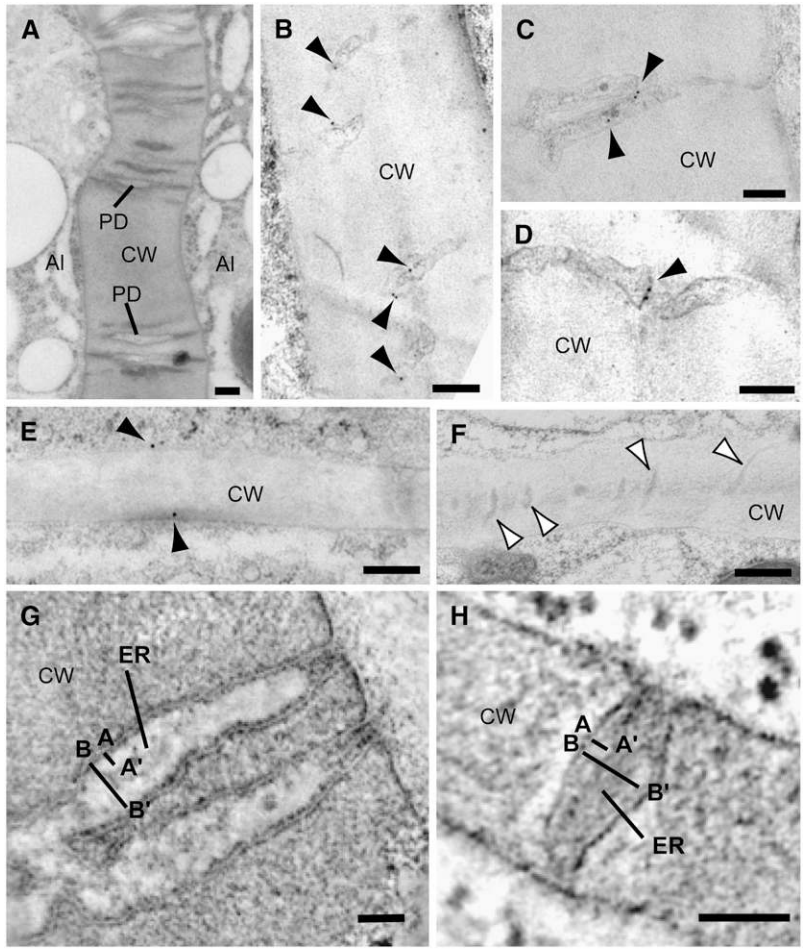

Figure 7. Electron Microscopy Analysis of CR4 Localization in Maize.

(A) General overview of branched plasmodesmata (PD) connecting aleurone cells in a high-pressure frozen/freeze-substituted in vitro–grown maize endosperm. Al, aleurone; CW, cell wall.

(B) to **(D)** Immunogold labeling of CR4 (GR2 antibodies) on plasmodesmata (arrowheads) between aleurone cells.

(E) and **(F)** Immunogold labeling of CR4 on the plasma membrane (black arrowheads in **[E]**) of starchy endosperm cells. The plasmodesmata connecting starchy endosperm cells (white arrowheads in **[F]**) are much narrower than those located between aleurone cells and showed very low or no CR4 labeling.

(G) and **(H)** Tomographic slices of plasmodesmata in cell walls between aleurone cells **(G)** and between starchy endosperm cells **(H)**. Line A to A′ indicates the distance between the plasma membrane and the endoplasmic reticulum membrane (ER), and line B to B′ indicates the widest total diameter of the plasmodesmata.

Bars = 100 nm in **(A)** to **(F)** and 50 nm **(G)** and **(H)**.

distribution of plasmodesmata (Figures 7G and 7H). The aleurone cells contained wide and branched plasmodesmata in anticlinal cell walls (Figures 7A and 7G). On average, the inner maximum diameter of plasmodesmata connecting aleurone cells was 62 ± 5 nm ($n = 9$) and the distance between the plasma membrane and the endoplasmic reticulum membrane was ~20 nm (Figure 7G). By contrast, plasmodesmata between starchy endosperm cells were mostly unbranched and much narrower (inner maximum diameter average was 41 ± 4 nm, and plasma membrane-to-endoplasmic reticulum membrane distance was 10.5 nm [$n = 14$]) (Figure 7H) than those connecting aleurone cells. These observations show variation in the distribution and structure of plasmodesmata in endosperm, suggesting a greater symplastic communication between aleurone cells than between starchy endosperm cells. The plasmodesmata connecting aleurone and starchy endosperm cells show intermediate features between those connecting aleurone cells and those connecting starchy endosperm cells.

Differentiating Aleurone Cells Establish a Symplastic Subdomain

To test for the presence of more than one symplastic domain established by plasmodesma connections in the developing

maize endosperm, we incubated in vitro–grown endosperm with two fluorescent tracers, the small 524-D tracer 8-hydroxypyrene-1,3,6-trisulfonic acid (HPTS) and 40-kD dextran conjugated to FITC (40kD-F-dextran) (Kim et al., 2002). In endosperms grown in vitro for 2 and 5 d, HPTS moved through all endosperm cells (Figures 8A and 8B). However, the 40kD-F-dextran tracer moved only through the aleurone cells, suggesting that the differentiating aleurone cells form a symplastic subdomain within the endosperm (Figures 8C to 8H). Interestingly, whereas the 40kD-F-dextran tracer moved through up to 90% of the aleurone cells in 2-d in vitro–grown endosperm, the same tracer was only able to move through up to 40% of the aleurone cells in the 5-d in vitro–grown endosperm. These results indicate that although symplastic connectivity between aleurone cells remained, as shown by the movement of the small HPTS tracer, the exclusion size of the plasmodesmata located between aleurone cells was reduced during endosperm development. Most of the aleurone cells containing the 40kD-F-dextran tracer in the 5-d in vitro–grown endosperm were located at young bulges or miniendosperms (Figure 8F) that formed by localized high mitotic activity (Gruis et al., 2006).

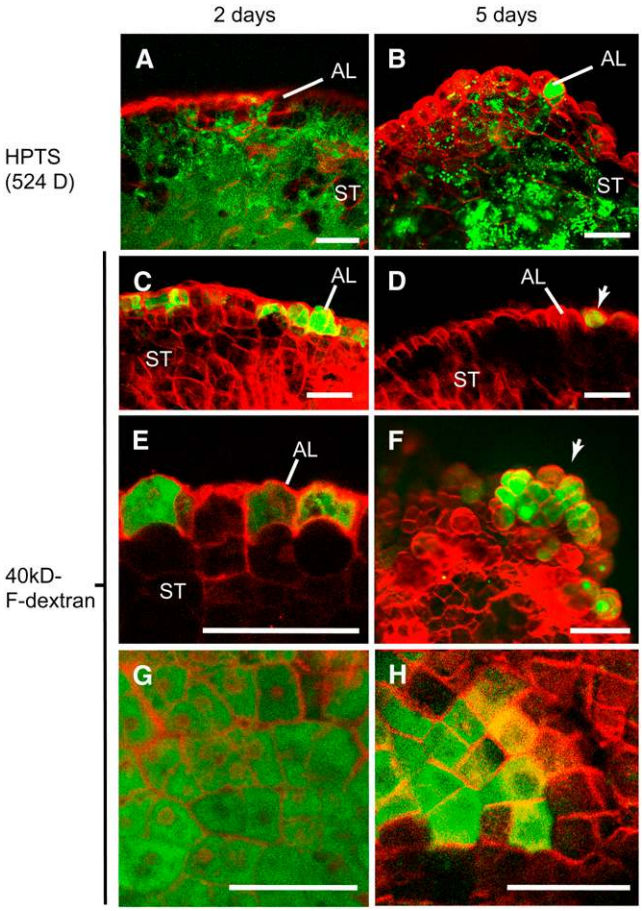

Figure 8. Cell-to-Cell Movement of Fluorescent Tracers in in Vitro–Grown Maize Endosperms.

(A) and **(B)** Endosperms grown in vitro for 2 d **(A)** or 5 d **(B)** allow the movement of HPTS through both differentiating aleurone (AL) and starchy endosperm (ST) cells.

(C) to **(H)** In vitro–grown endosperm incubated in 40 kD of F-dextran. The tracer is able to move only through the aleurone cells of endosperms cultured for 2 d (**[C]**, **[E]**, and **[G]**) or 5 d (**[D]**, **[F]**, and **[H]**), but the movement is highly reduced in the latter. Most of the aleurone cells that contain the 40-kD F-dextran in the 5-d-in-culture endosperms are located at growing bulges at the endosperm surface (**[F]**, arrow). **(G)** and **(H)** show paradermal views of the aleurone layer in endosperms grown in vitro for 2 d **(G)** or 5 d **(H)**. Note the reduction in the aleurone cells containing the 40-kD F-dextran tracer in the older endosperms.

Bars = 100 μm.

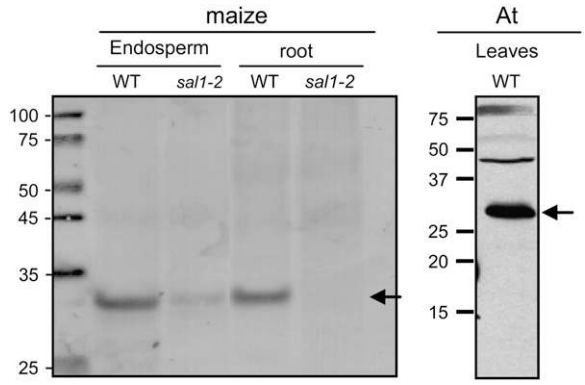

Figure 9. Characterization of SAL1 Antibodies.

Immunoblots of protein extracts from maize wild type and *sal1-2* mutant endosperms and roots as well as *Arabidopsis* leaf proteins (At) probed with anti-SAL1 antibodies. Arrows show bands at the predicted size for SAL1. The presence of a weak band in the mutant shows that the maize *sal1-2* mutant is not a null allele.

SAL1 Colocalizes with DEK1 and CR4 in Endosomes

The data presented above suggested that DEK1 and CR4 colocalize in endosomes. Therefore, we investigated whether these endosomes associate with the SAL1 protein. Immunoblot analysis of maize protein extracts from wild-type endosperm showed that polyclonal rabbit antibodies against recombinant SAL1 protein recognized a protein of ~27 kD, the expected size for SAL1 (Figure 9, left panel). In extracts from *sal1-2* mutant endosperm, the band was weaker, suggesting that the *sal1-2* allele was not a null allele. The maize SAL1 antibody also recognized a protein with the expected size for At SAL1 (~27.5 kD) (Figure 9, right panel). Two weaker bands of higher molecular mass were also recognized by the antibody in *Arabidopsis* extracts. Furthermore, the anti-SAL1 antibody labeled multivesicular bodies (endosomes) in *Arabidopsis* embryo cells, confirming that SAL1 localizes to endosomal compartments, as predicted based on its high amino acid identity to class E vacuolar proteins such as CHMP1 and DID2 (Figures 10A to 10C).

Next, we used the SAL1 antibody to immunolabel sections of in vitro–grown maize endosperm. As shown in Supplemental Figure 4A online, SAL1 is present in small structures distributed throughout the cytoplasm in both aleurone and starchy endosperm cells from wild-type plants. There was no difference in the

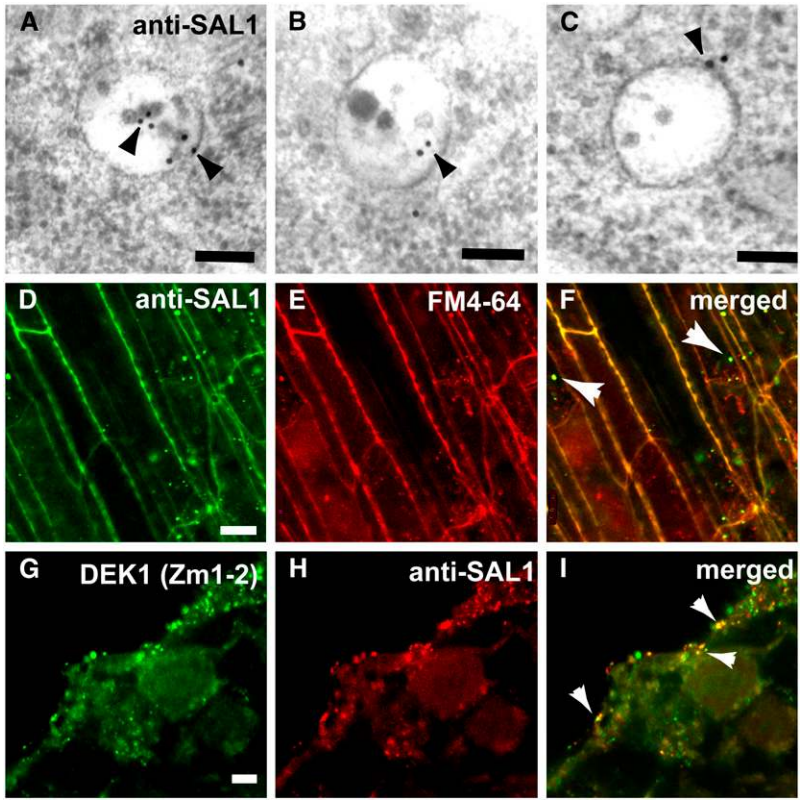

Figure 10. Localization of SAL1 in *Arabidopsis* and Maize Cells.

(A) to **(C)** Immunogold labeling of multivesicular endosomes in high-pressure frozen/freeze-substituted *Arabidopsis* embryo cells with anti-SAL1 antibodies. The antibodies labeled 60% of the multivesicular bodies analyzed ($n = 40$).

(D) to **(F)** Colocalization of SAL1 and the endocytotic marker FM4-64 in punctate structures, likely endosomes (arrowheads in **[F]**), in wild-type maize roots. **(D)** shows immunolabeling with anti-SAL1 antibodies and a FITC-conjugated secondary antibody, and **(E)** shows staining with fixable FM4-64. **(F)** shows a merged image of **(D)** and **(E)**.

(G) to **(I)** In vitro endosperm section immunostained with DEK1 rat antibody Zm1-2 **(G)** and SAL1 **(H)**. Overlapping staining **(I)** is indicated by arrowheads in the merged image of **(G)** and **(H)**.

Bars = 10 μm.

distribution of SAL1 signal between aleurone and starchy endosperm (data not shown), nor could we detect a difference in the distribution of SAL1 between wild-type and *sal1-2* mutant endosperms (see Supplemental Figure 4B online). This observation is not surprising in light of the fact that *sal1-2* is not a null allele. As reported above, we used maize roots for our FM4-64 labeling experiments. In this system, double labeling with FM4-64 and the maize SAL1 antibody confirmed the presence of SAL1 in endosomes (Figures 10D to 10F). To determine whether the *sal1-2* mutation affected the pattern of localization of DEK1 and CR4, we also immunostained *sal1-2* in vitro–grown endosperm with DEK1 Zm8 and CR4 GR2 antibodies and found no obvious difference between wild-type and *sal1-2* mutant endosperm (see Supplemental Figures 4C and 4D online).

Finally, we investigated whether SAL1 colocalizes with CR4 and DEK1. To test for DEK1 and SAL1 colocalization, we immunolabeled wild-type maize endosperms with the DEK1 Zm1-2 antibodies (Figure 10G) followed by the SAL1 antibodies (Figure 10H). We observed extensive colocalization on small cytoplasmic structures, likely endosomes (Figure 10I). Next, we localized CR4 by GFP fluorescence from the fusion protein CR4:HA:FLAG:AcGFP and then SAL1 by immunolabeling of the same section of in vitro–grown endosperm (see Supplemental Figures 5A to 5C online). The results supported the conclusion that SAL1 colocalized with DEK1 and CR4 in endosomes of maize endosperm.

DISCUSSION

DEK1 Plays a Conserved Role in Epidermis Cell Fate Specification

As demonstrated by the lack of aleurone cells in in vitro–grown *dek1* mutant endosperm (Gruis et al., 2006), DEK1 plays an essential role either in the perception and/or in the transmission of the positional cue initiating the epidermal cell fate. From the observation of similar epidermal *dek1* mutant phenotypes in maize and *Arabidopsis*, both in seeds and in vegetative organs, we infer that the role of DEK1 in epidermal cell fate specification is

conserved and that both systems provide valuable insight into DEK1 function. The remarkable sequence conservation of DEK1 over the course of land plant evolution, as indicated by the high degree of similarity between angiosperm and moss protein sequences, also suggests a conserved role for DEK1.

In maize in vitro cultures, interior starchy endosperm cells that become positioned adjacent to internal voids that occasionally develop convert to aleurone cells (Gruis et al., 2006). A prerequisite for a protein postulated to respond to such positional information is that it is ubiquitously distributed in all cells. This important criterion is fulfilled for DEK1, as shown by in situ hybridization experiments and high-resolution transcript profiling in maize and *Arabidopsis* (Lid et al., 2005). The data showing ubiquitous distribution of DEK1 in peripheral and internal cell layers of in vitro endosperm presented here also support this conclusion.

DEK1-CALP Fails to Fully Complement the *dek1* Mutant Phenotype

We previously proposed that DEK1 is activated by external signaling and that this activity is transmitted via the protease activity of DEK1-CALP. This hypothesis was based on the highly conserved active site of DEK1 compared with typical animal calpains as well as on the fact that DEK1-CALP displays calpain Cys proteinase activity in vitro (Wang et al., 2003). Here, we have shown that maize DEK1-CALP failed to complement the loss-of-aleurone cell phenotype in homozygous maize *dek1* mutant endosperm under the control of the 27-kD γ-*Zein* promoter. Since DEK1-CALP possesses proteinase activity in vitro (Wang et al., 2003), we infer that DEK1 calpain activity is present in the peripheral cells of the transgenic endosperm expressing DEK1-CALP. In spite of this, the peripheral cell layer of the endosperm failed to assume an aleurone cell fate. The expression of At DEK1-CALP also failed to fully complement the *Arabidopsis dek1* mutant phenotype. These results support the conclusion that DEK1-MEM is necessary for wild-type DEK1-CALP activity.

Recently, the membrane-bound transcription factor NTM1 (for NAC WITH TRANSMEMBRANE MOTIF1) was identified as a putative substrate for DEK1 in *Arabidopsis* (Kim et al., 2006). This conclusion was supported by the similar phenotypes of *Arabidopsis* plants that overexpress the *Arabidopsis DEK1* gene and *ntm1-D* mutant plants (Kim et al., 2006). In addition, the calpain inhibitor *N*-acetyl-leucinyl-leucinyl-norleucinal inhibits NTM1 processing, suggesting that NTM1 may be released from the membrane by the DEK1 calpain protease. Future experiments should reveal whether or not NTM1 is a substrate of DEK1.

Overexpression of At DEK1-MEM Gives a Dominant Negative Phenotype

Ectopic expression of At *DEK1*-MEM under the control of *CaMV35S* in *Arabidopsis* gives a phenotype that closely resembles the mutant phenotype seen in At *DEK1*-RNAi suppression lines. One explanation for the dominant negative phenotype caused by DEK1-MEM overexpression is that DEK1-MEM interacts with either a ligand or interacting membrane proteins that normally mediate the activation of DEK1. The overexpressed DEK1-MEM truncated protein competes with native DEK1 for the DEK1 activators and/or interactors, and since it lacks the cytoplasmic calpain domain, it cannot trigger the downstream signaling pathways, leading to a dominant negative phenotype. The observation that expression of At DEK1-MEM under the weaker At *DEK1* promoter fails to give a detectable phenotype suggests that a threshold level of truncated protein has to be surpassed to interfere with the endogenous DEK1 protein function. The observation that plants overexpressing At DEK1-MEM-DEL, which lack the loop region (Figure 1A), display a phenotype indistinguishable from the wild type strengthens the conclusion that the observed dominant negative phenotype is specific to DEK1-MEM. Furthermore, this observation supports the speculation that the loop region is essential for either the perception and/or the transmission of positional signals.

The nature of the signal for epidermal cell fate specification is unknown. We previously speculated that that epidermal cell fate specification is suppressed internally in the endosperm by lateral inhibition from neighboring cells and that this inhibition is only escaped in the outer membrane/cell wall of cells exposed to the surface. Since the dominant negative phenotype caused by At DEK1-MEM overexpression suggests that DEK1 is activated at the plasma membrane, likely by an extracellular signal, DEK1 may function downstream of the primary signal for surface or aleurone fate specification. A scenario in which DEK1 activation occurs by autodimerization also represents a possibility that cannot be ruled out. One way to identify putative DEK1 interactors is by yeast two-hybrid experiments using the different predicted extracellular loop regions as baits. The design of these studies, however, is hampered by the lack of insight into the three-dimensional structure of DEK1, which may form a pore or a channel-like structure in the membrane. Therefore, interaction by extracellular molecules or other transmembrane proteins may be with several DEK1 domains simultaneously, a situation that is difficult to recreate in yeast two-hybrid screens.

DEK1 and CR4 Colocalize in SAL1-Positive Endosomes

In addition to the plasma membrane, DEK1 localized to membranous structures that we interpret to be endosomes. Recently, Johnson et al. (2005) presented data showing that GFP-tagged ACR4 in *Arabidopsis* root cells was present in two distinct subcellular compartments: protein export bodies or secretory vesicles and a population of internalized vesicles or endosomes. The authors concluded that internalization and turnover for ACR4 are linked and depend on functionality, suggesting that ACR4 signaling may be subject to downregulation via internalization. In their experiments with *Arabidopsis* root epidermal cells, identification of endocytic/endosomal compartments was based on FM4-64 incubation experiments. Using maize roots, we show here that FM4-64–positive compartments also stained positive for SAL1. The observation that SAL1-positive compartments are stained by FM4-64 after 15 min of incubation strongly supports the conclusion that these structures represent endosomal compartments. In addition, the fact that the maize SAL1 antibodies recognized epitopes in multivesicular bodies in *Arabidopsis* embryos also supports this conclusion.

In the same experiments, we also demonstrated that DEK1- and CR4-positive organelles stained positive with FM4-64, leading us to speculate that DEK1 and CR4 are both internalized by endocytosis and routed through endosomal compartments. The functional significance of an internalization process has yet to be determined, but a quantitative regulation of vital cellular receptors by endosomal degradation is common in animal systems, including animal growth hormone receptors (Mellman, 1996; Katzmann et al., 2002). As demonstrated by the presence of extra layers of aleurone cells in the maize *sal1-2* mutant, SAL1 is a negative regulator of aleurone cell fate. In animal systems, the SAL1 homolog CHMP1 mediates the trafficking of cargo proteins from multivesicular bodies to lysosomes for degradation (Howard et al., 2001). We earlier proposed that the supernumerary aleurone layer phenotype of *sal1* mutants is caused by an overabundance of positive regulators of aleurone cell fate due to defective degradation via endosomes. The data presented here support this proposal in two ways. First, by demonstrating that SAL1 localizes to endosomes, and second, by demonstrating that SAL1 colocalizes with the two known regulators of aleurone cell fate, DEK1 and CR4. The immunolocalization experiments performed here did not show differences between the distribution of DEK1 and CR4 in wild-type and *sal1-2* mutant endosperms. We ascribe this observation to the fact that the *sal1-2* mutant is not a null mutant, the protein being present in mutant endosperm at a reduced level compared with the wild type. Nevertheless, *sal1-2* mutant endosperms display multiple layers of aleurone cells in in vitro organ cultures (Gruis et al., 2006). Therefore, we speculate that the multiple aleurone layer phenotype of *sal1* mutants is caused by an overabundance of aleurone signaling membrane proteins (e.g., DEK1 and CR4).

Aleurone Cells of Young Endosperm Form a Symplastic Subdomain through Wide Plasmodesmata Enriched in CR4

The localization pattern of CR4 in maize endosperm and roots shown in this study is in agreement with data presented by Johnson et al. (2005) on *Arabidopsis* root cells. These data support the notion that CR4 is present in many different cell types across monocot and dicot species and that targeting, function, and regulation may be the same in all of these cells. In *Arabidopsis* root cells, the ACR4 has been described as an L1 cell layer–specific kinase (Johnson et al., 2005). This conclusion is not supported by our data from endosperm, in which CR4 was shown to be expressed in all cell layers. Interestingly, however, CR4 is primarily associated with plasmodesmata only in the aleurone layer and not in the starchy endosperm. Whether the preferential presence of CR4 in periclinal epidermal cell walls of *Arabidopsis* leaf primordia and ovules (Tanaka et al., 2002; Gifford et al., 2003) also reflects an association with specialized plasmodesmata remains to be determined. The CR4-positive plasmodesmata in anticlinal walls of aleurone cells show a larger inner diameter and also exhibit a larger plasmodesmata exclusion size, leading to the development of symplastic subdomains of aleurone cells in young endosperm, as demonstrated by the movement of fluorescent tracers. The association of CR4 with these plasmodesmata

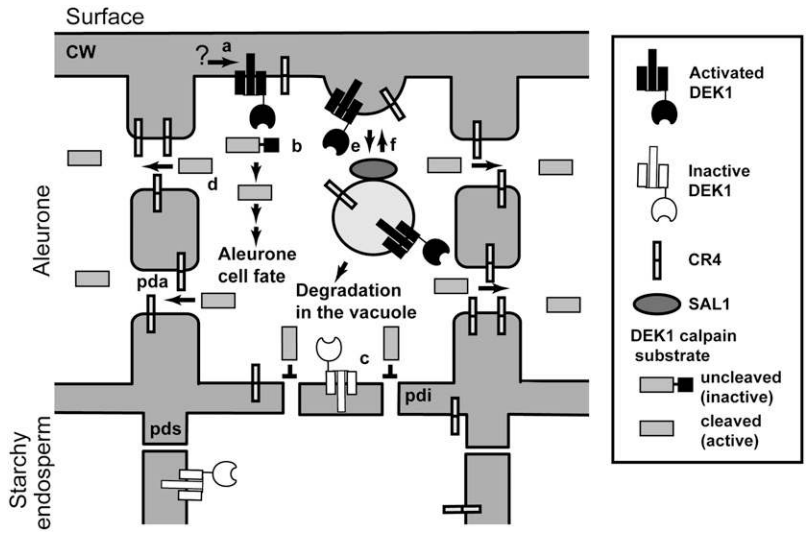

Figure 11. A Model for the Role of DEK1, CR4, and SAL1 in Aleurone Cell Specification.

DEK1 at the surface of the endosperm is activated by an unknown mechanism (a), its calpain domain in the cytosol cleaving a postulated substrate (b) that leads to the specification of aleurone cell fate. DEK1 in all other positions is inactive (c). In cells with active DEK1 signaling, CR4 concentrates on plasmodesmata between aleurone cells (pda) and increases the plasmodesma exclusion limit, allowing the activated DEK1 substrate to move laterally between aleurone cells, thereby reinforcing the signal for aleurone cell fate specification (d). Plasmodesmata in cell walls between starchy endosperm cells are narrow (pds), whereas plasmodesmata in cell walls between aleurone cells and starchy endosperm cells are intermediary in width (pdi). DEK1 and CR4 are internalized by endocytosis (e) and traffic through endosomes. Whereas some DEK1 and CR4 molecules may be recycled back to the plasma membrane (f), others are sorted for degradation in the vacuole in a process that requires SAL1. Some endosomes are recycled back to the plasma membrane (f).

places CR4 downstream of DEK1 in aleurone signaling, a conclusion that is in agreement with previous observations in *Arabidopsis* embryos (Johnson et al., 2005).

Although the establishment of symplastic domains during plant development has been well documented in previous studies (Kim et al., 2002), one possibility that we raise here is that CR4 may be involved in increasing the exclusion limit for molecules moving laterally between aleurone cells, in particular the activated substrate of DEK1 or a molecule downstream of this substrate. If correct, the relative importance of this activity on aleurone cell fate specification may be revealed by the phenotype of homozygous *cr4* mutant endosperms, in which ~10% mutant kernels show mosaic aleurone layers (Becraft et al., 1996). One interpretation is that sectors on the endosperm surfaces lacking aleurone cells represent symplastic subdomain(s) in which lateral transmission of the signal activating aleurone cell fate specification failed due to a lack of CR4 activity. Interestingly, different *cr4* mutants show distinct patterns of failure to develop aleurone cells, ranging from the absence of aleurone cells in the abgerminal region of the kernel to the absence in mainly germinal regions (Becraft and Asuncion-Crabb, 2000). In addition, several other mutants that disrupt aleurone differentiation also display distinct mosaic aleurone phenotypes, including *bareback* and *naked* (Becraft and Asuncion-Crabb, 2000). Based on the results shown here, one possible explanation for these phenotypes is that they are affected in functions needed to establish or maintain aleurone symplastic subdomains. It is also interesting that Becraft and coworkers (2001) concluded from their *cr4* mutant sector studies that although CR4 appears to function cell autonomously, the phenotype of several sectors with *cr4* mutant cells appeared defective in the production of lateral developmental signals. Finally, a protein kinase that recognizes a specific subset of viral as well as endogenous proteins associated with plasmodesmata has already been identified in plants (Lee et al., 2005).

Summary: A Model for Aleurone Cell Fate Specification

Aleurone cell fate specification in maize endosperm occurs exclusively in response to surface position, a process that involves the function of DEK1, CR4, and SAL1. The data presented here show that DEK1 and CR4 are located at the plasma membrane and in SAL1-positive endosomes in all cells investigated. Based on these and earlier observations, we propose a model for aleurone cell fate specification in which in DEK1 is active only in the outer membrane of cells positioned on endosperm surfaces (Figure 11). To be fully functional, the calpain activity must be under the control of the membrane portion of DEK1, in which the loop region plays an essential functional role. The DEK1 substrate may be a cytoplasmic protein or, as suggested by Kim et al. (2006), a membrane-bound transcription factor such as NTM1. Once aleurone cell fate specification has been initiated, the process is reinforced via lateral signaling in symplastic subdomains mediated by CR4 in specialized plasmodesmata. Finally, we predict that the proper plasma membrane concentration of DEK1 and CR4 is maintained by internalization and degradation at SAL1-positive endosomes. We also hypothesize that this model is valid for epidermal cell fate specification in all plants and that DEK1 was recruited early during land plant evolution to serve in this role.

METHODS

Plant Material, Growth Conditions, and Generation of Transgenic Plants

Maize (*Zea mays*) plants were grown under typical greenhouse conditions (68 to 82°F, 16 h of light/8 h of dark) using a commercial potting medium (Metro-Mix 700; Scotts-Sierra) and fertilized as needed with a standard fertilizer mixture (20:10:20 N:P:K). Two to 3 d after the first silks appeared, pollination was performed to prepare material for in vitro endosperm cultures. Maize in vitro endosperms were grown as detailed by Gruis et al. (2006). For immunostaining of maize roots, maize seeds were sandwiched in four layers of wet paper towels and placed on a glass plate at room temperature. Three days after germination, root tissues were harvested and processed for immunostaining. For immunoblot analyses, 12-DAP *dek1*/*dek1* and *Dek1* (wild-type) kernels from *Dek1*/*dek1* ears were frozen in liquid nitrogen for storage at −80°C until use. Roots from *cr4*/*cr4* and wild-type plants were frozen at the V3 stage in liquid nitrogen for storage at −80°C until use.

All *Arabidopsis thaliana* lines were produced in the Columbia ecotype. *Arabidopsis* plants were grown in growth chambers at 22°C and 70% humidity under cool-white fluorescent light (85 μmol m^{-2} s^{-1}) for 8 h of dark and 16 h of light. Constructs were transformed into the *Agrobacterium tumefaciens* strain C58C1 pGV2260 (Deblaere et al., 1985) by electroporation. *Arabidopsis* plants were transformed by a modified version of the floral dip method (Clough and Bent, 1998), in which the *Agrobacterium* culture was applied directly to flower buds using a pipette. Transformants were selected on Murashige and Skoog (1962) medium containing 50 μg/mL kanamycin.

Antibody Production and Purification

Polyclonal antibodies against DEK1, CR4, and SAL1 were raised in rabbits or rats and affinity-purified according to the manufacturer's manual. For DEK1, we raised the antibodies against the following peptides: Zm1 and Zm1-2, 5′-KGERNFTDQEFPPEDR-3′; ZM3, 5′-VREVDGHKL-3′; ZM6, 5′-PFVLSVFSKASIRLEAV-3′; Zm8, 5′-DKGLDPNFSYMLKDK-3′; and ZM9, 5′-LYKWKDDDWKISR-3′. DEK1 rabbit antibodies were used at dilutions of 1:3000 for immunoblot analyses and 1:300 for immunostaining. DEK1 rat antibody was used at dilutions of 1:3000 for immunoblot analyses and 1:200 for immunostaining. For CR4, antibodies were raised against peptides in the external domain (GR2, 5′-MTATHAVDEAVS-3′) and in the internal domain (GR8, 5′-YRAPSWITFPSVTSSQRR-3′). CR4 antibodies were used at dilutions of 1:5000 for immunoblot analyses and 1:300 for immunostaining. SAL1 antibody was raised against the whole protein and used at dilutions of 1:5000 for immunoblot analyses and 1:500 for immunostaining. Antibodies against HA (Sigma-Aldrich; catalog number H9658) and FLAG (Sigma-Aldrich; catalog number F3165) were used at dilutions of 1:15,000 for immunoblot analyses and 1:1500 for immunostaining. Antibody against GFP (BD Living Colors; catalog number 632380) was used at a dilution of 1:3000 for immunoblot analyses.

Plasmid Construction and Plant Transformation

To construct Zm DEK1-CALP:HA:FLAG:AcGFP, *Dek1* cDNA from maize (GenBank accession number AY061805; nucleotides 3683 to 6532) was fused to cDNA for HA (amino acid sequence TSYPYDVPDYA), FLAG (amino acid sequence DYKDDDDK), and the GFP gene (Clontech) from *Aequorea coerulescens* downstream of the maize 27-kD γ-*Zein* promoter (1473 bp) isolated from the W64A maize line (Ueda and Messing, 1991; Russell and Fromm, 1997). Several linker sequences were used that generated the following amino acid sequences when translated: between the γ-*Zein* promoter and Zm *DEK1*-CALP, IGSEFELRRQ; between Zm Dek1-CALP and HA, DV; between HA and FLAG, QL; between FLAG and

AcGFP, A. For CR4:HA:FLAG:AcGFP expression, EST clsmc27 from maize (GenBank accession number U67422; nucleotides 157 to 2859) was fused to HA, FLAG, and AcGFP (as described above for Zm DEK1-CALP:HA:FLAG:AcGFP expression) downstream of the maize 27-kD γ-*Zein* promoter (1473 bp) isolated from the W64A line. The linkers used also generated extra amino acids in this construct: between CR4 and HA, DV; between HA and FLAG, QL; between FLAG and AcGFP, A. These constructs were transformed into maize embryos as described (Zhao and Ranch, 2006). T1 kernels were analyzed for fluorescence protein expression or protein expression on immunoblots.

Constructs for the transformation of *Arabidopsis* were prepared in the modified pCAMBIA2300 binary vectors pSEL1-Pro$_{CaMV35S}$ -NOS or pSEL1-NOS (Lid et al., 2005). All subclones derived by PCR amplification were initially cloned in pCR4-TOPO (Invitrogen) and sequenced using the BigDye Terminator version 3.1 cycle sequencing kit and the ABI PRISM 3100 genetic analyzer (Applied Biosystems) before cloning into their respective binary vectors. The genomic region corresponding to At DEK1-MEM was PCR-amplified from *Arabidopsis* genomic DNA of the Columbia ecotype using primers 5′-CCGGGCATGGAAGGGGATGAGC-GAGGAGTCTT-3′ and 5′-ACTAGTCTAAATTATCAGACTAGCAACAAC-ACCCCA-3′ that introduced a unique *Xma*I site immediately upstream of the ATG start site and a novel TAG stop codon at bp positions 5257 to 5259 relative to the ATG start as well as a *Spe*I site immediately 3′ to this stop codon. At *DEK1*-MEM was then cloned using *Xma*I and *Spe*I between *CaMV35S* and the *NOS* terminator in pSEL1- Pro$_{CaMV35}$-NOS.

In order to produce a C-terminal fusion of At *Dek1*-MEM and GFP, the 851-bp 3′ part of At *Dek1*-MEM was PCR-amplified from pSEL1-Pro$_{CaMV35}$-At *Dek1*-MEM-NOS using 5′-CTCTCGAGGTGTATATGTT-TTCTTTTCAAT-3′ containing an integral *Xho*I site and 5′-GGATCCAAT-TATCAGACTAGCAACAACACCCC-3′ introducing a *Bam*HI site in place of the stop codon and cloned into pCR4-TOPO (Invitrogen). The plasmid pKEx4tr-smGFP (a gift from Tage Thorstensen) was digested with *Bam*HI and *Spe*I, and the resulting GFP fragment was cloned into the 3′ end of At *Dek1*-MEM. The in-frame C-terminal fusion of GFP and the 3′ end of At *Dek1*-MEM was then cloned into At *Dek1*-MEM-pCR4-TOPO using *Xho*I and *Spe*I to give At *Dek1*-MEM-GFP-pCR4-TOPO. At *Dek1*-MEM-GFP was finally cloned into pSEL1-Pro$_{CaMV35}$-At *Dek1*-MEM-NOS using *Pst*I and *Spe*I to give pSEL1-Pro$_{CaMV35}$-At *Dek1*-MEM-GFP-NOS.

For overexpression of the At *DEK1*-RNAi construct, a 590-bp At *DEK1* cDNA fragment was first PCR-amplified from *Arabidopsis* Columbia cDNA isolated from seedlings using oligo(dT) dynabeads (Invitrogen) with the two primer sets 5′-CCCGGGACAAGAGCATCCTGAACCAGTC-3′/5′-GTCGACAGGAAACCCAGGATGGAGA-3′and 5′-ACTAGTACAGG-AAACCCAGGATGGAGA-3′/5′-GGTACCGACAAGAGCATCCTGAAC-CAGTC-3′, introducing 5′ *Xma*I and 3′ *Sal*I sites to one copy and 5′ *Kpn*I and 3′ *Spe*I sites to the other copy. The 190-bp *Catalase* intron from the *GUS* gene in pCAMBIA2301 (AF234316) was PCR-amplified using primers 5′-GTCGACGGGTAAATTTCTAGTTTTTCTCC-3′ and 5′-ACT-AGTGGTTCTGTAACTATCATCATCATC-3′, introducing 5′ *Sal*I and 3′ *Spe*I sites. The *Xma*I/*Sal*I and *Kpn*I/*Spe*I cDNA copies of At *DEK1* as well as the *Sal*I/*Spe*I clone of the *Catalase* intron were cloned between *CaMV35S* and the *NOS* terminator in pSEL1-Pro$_{CaMV35}$-NOS using the added restriction sites, resulting in inverted repeats of the At DEK1 cDNA fragment flanking the *Catalase* intron.

The 2.6-kb At DEK1 promoter was PCR-amplified from *Arabidopsis* genomic DNA of the Columbia ecotype using primers 5′-GGATCCAA-GAGGGACACTGGTGGATGCAATTTG-3′ and 5′-CCCGGGCTTCTTCT-CCCACCTACAACACCATGCA-3′, introducing a 5′ *Bam*HI site and a 3′ *Xma*I site immediately upstream of the ATG start codon. pSEL1-ProCamV35S-At DEK1-CALP-NOS was digested with *Sal*I and *Kpn*I, and the resulting *DEK1*-CALP fragment was cloned between the At *DEK1* promoter and the *NOS* terminator in pSEL1-Pro$_{AtDEK1}$-NOS. At *DEK1*-CALP was PCR-amplified from *Arabidopsis* Columbia cDNA isolated from seedlings using oligo(dT) dynabeads (Invitrogen) with primers 5′-CCCG-GGCATGTGTGCCCATGCAAGAGTT-3′ and 5′-GGTACCTGACAATAC-GGGCACTACAAAGCT-3′, adding a 5′ *Xma*I site and a 3′ *Kpn*I site, with which At *DEK1*-CALP was cloned between the At *DEK1* promoter and the *NOS* terminator in pSEL1-Pro$_{AtDEK1}$-NOS. In order to produce a C-terminal fusion of At *DEK1*-CALP and FLAG (amino acid sequence DYKDDDDK), the 903-bp 3′ part of At *DEK1*-CALP was PCR-amplified from pSEL1-Pro$_{AtDEK1}$-At *Dek1*-CALP-NOS using 5′-GGACTGGTTCAG-GATGCTCTTGT-3′, containing an integral *Sal*I site, and 5′-GGTAC-CCTACTTGTCATCGTCGTCCTTGTAGTCCAAAGCTTCAAGAACAATGG-ATGCT-3′, introducing FLAG, a stop codon, and a new *Kpn*I site in place of the old stop codon, and cloned into pCR4-TOPO (Invitrogen). The in-frame C-terminal fusion of the 3′ end of At *Dek1*-CALP was finally cloned into pSEL1-Pro$_{AtDEK1}$-At *DEK1*-CALP-NOS using *Sal*I and *Kpn*I to give pSEL1-ProAt DEK1-At DEK1-CALP:FLAG-NOS.

In order to replace the loop domain of At Dek1-MEM with the transmembrane linker domain of At *Dek1* exon 11 (amino acid sequence RFSHSSA), the fragment was PCR-amplified from pSEL1-Pro$_{CaMV35}$-At *Dek1*-MEM-NOS using two primer sets: 5′-GGAGGAATCACATCAG-CTGCAGT-3′, containing an integral *Pst*I site, and 5′-CTCGAGTGGGA-AAACCTTGGGTCTGTTATAGATAGATGCCGAG-3′, introducing a *Xho*I site; and 5′-CTCGAGTGCTCCAGAGAGAGCATGGGGCCT-3′, introducing a *Xho*I site, and 5′-GTGGGCAACTGATCATCTCTAGATTTTA-3′, containing an integral *Xba*I site. The two fragments were ligated in pCR4-TOPO, and the transmembrane linker was cloned into pSEL1-Pro$_{CaMV35}$-At *Dek1*-MEM-NOS using *Pst*I and *Xba*I, to give pSEL1-ProCaMV35-At Dek1-MEM-DEL-NOS.

In order to produce a C-terminal fusion of At Dek1-MEM-DEL and FLAG (amino acid sequence DYKDDDDK), the 1107-bp 3′ part of At *Dek1*-MEM was PCR-amplified from pSEL1-Pro$_{CaMV35}$-At *Dek1*-MEM-DEL-NOS using 5′-CGTGGCATTTTGTGGAACTTCA-3′, containing an integral *Xba*I site, and 5′-ACTAGTCTACTTGTCATCGTCGTCCTTGTAGTCAATTATC-AGACTAGCAACAACACCCCA-3′, introducing FLAG, a stop codon, and *Spe*I. The in-frame C-terminal fusion of the At *Dek1*-MEM-DEL 3′ end and FLAG was finally cloned into pSEL1-Pro$_{CaMV35}$-At *Dek1*-MEM-DEL-NOS using *Xba*I and *Spe*I, to give pSEL1-Pro$_{CaMV35}$-At *Dek1*-MEM-DEL:FLAG-NOS. In order to produce a C-terminal fusion of At *Dek1*-MEM-DEL:FLAG and 6xHIS, the 3′ part of At *Dek1*-MEM-DEL:FLAG was PCR-amplified using 5′-CGTGGCATTTTGTGGAACTTCA-3′, containing an integral *Xba*I site, and 5′-ACTAGTCTAGTGATGGTGATGGTGATGCTTGTCATCGT-CGTCCTTGTAGTCA-3′, introducing 6xHIS, a stop codon, and *Spe*I. The in-frame C-terminal fusion of the At *Dek1*-MEM-DEL:FLAG 3′ end and the His tag was finally cloned into pSEL1-Pro$_{CaMV35}$-At *Dek1*-MEM-DEL-NOS using *Xba*I and *Spe*I, to give pSEL1-Pro$_{CaMV35}$-At *Dek1*-MEM-DEL:FLAG-HIS-NOS. In order to produce an N-terminal fusion of At *Dek1*-MEM-DEL and FLAG, the 5′ part of At *Dek1*-MEM was PCR-amplified from pSEL1-Pro$_{CaMV35}$-At *Dek1*-MEM-DEL-NOS using 5′-CCCGGGATGGACTACAAGGACGACGATGACAAGATGGAAG-GGGATGAGCGAGG-3′, introducing *Xma*I, a start codon, and FLAG, and 5′-CCAAGAACAATAACTGCAGCTGATG-3′, containing an integral *Pst*I site. The in-frame N-terminal fusion of the At *Dek1*-MEM-DEL 5′ end and FLAG was then cloned into pSEL1-Pro$_{CaMV35}$-At *Dek1*-MEM-DEL-NOS using *Xma*I and *Pst*I, to give pSEL1-Pro$_{CaMV35}$-FLAG:At *Dek1*-MEM-DEL-NOS.

RT-PCR Analyses

Isolation of poly(A)$^+$ RNA from 35S-Dek1-MEM, 35S-Dek1-RNAi, and wild-type control seedlings, as well as first-strand cDNA synthesis and PCR conditions, were as described previously (Lid et al., 2005). To ensure that amplification was in the logarithmic phase, the smallest number of PCR cycles allowing detection on an ethidium bromide–stained agarose gel was experimentally calculated and used. The number of cycles used was 28 in Figure 4A and 29 in Figure 4B. All PCRs were performed at 57°C annealing temperature. The primer pairs used were as follows: At

Dek1-MEM, 5′-TTTGGGCTGTTAATTGGCGG-3′ and 5′-CAACGTGATTCCCTAGCTGTGAGA-3′; At Dek1-CALP, 5′-CAACGTGATTCCCTAGCTGTGAGA-3′ and 5′-ACTCCGCAAGTCAATCTCCTCA-3′; EF-1α, 5′-CACATCAACATTGTGGTCATTGG-3′ and 5′-GGTAGTGGCATCCATCTTGTTACAA-3′.

Immunoblot Analysis

Frozen wild-type and mutant materials were ground with a mortar and pestle in liquid nitrogen. Equal fresh weights of the samples were ground again with a plastic pestle in extraction buffer (50 mM Tris-HCl, pH 8.0, at 25°C, 5 mM EDTA, and 2% SDS) with 1× protease inhibitor (Sigma-Aldrich) at a 1:2 (w/v) ratio. Cellular debris was removed by centrifugation at 140,000 rpm for 10 min. Protein extracts were diluted 1:2 (v/v) in sample buffer and boiled for 5 min before separation through a 4 to 12% (w/v) SDS polyacrylamide gel (Invitrogen) and then transferred to a cellulose membrane in a submerged blotting system (Mini-Trans Blot; Invitrogen). Membranes were blocked for 1 h with Tris-buffered saline containing 5% (w/v) nonfat dry milk. Immunoblotting of DEK1 was performed using Zm1 and anti-rabbit secondary antibodies (Bio-Rad Laboratories) in Tris-buffered saline containing 0.1% (v/v) Tween 20. Immunoblotting of CR4 was performed using GR2 and GR8 antibodies. Proteins that cross-reacted with antibodies were detected with chemiluminescent substrates (Pierce) and visualized on x-ray film.

Fluorescence Immunolabeling

Endosperms were fixed in 4% paraformaldehyde overnight at 4°C, sectioned at 60 μm using a vibratome, and placed on cover slips with a thin layer of Meyer's adhesive (50% egg white and 50% glycerol). After dying, the sections were covered with a film of 0.75% low-melting-point agarose and 0.75% gelatin in double-distilled water. After three washes with PHEM/DMSO (50 mM PIPES, 5 mM EGTA, 1 mM $MgSO_4 \cdot 7H_2O$, pH 6.8, and 1% DMSO) buffer, the cover slips were incubated with 1% β-glucuronidase (Sigma-Aldrich) and 1% Pectolyase (Kikkoman) for 20 min at room temperature followed by 1% Triton X-100 for 10 min at room temperature to digest the cell wall. After three washes with PHEM/DMSO buffer, they were incubated with block buffer (3% BSA and 5% goat serum) for 1 h at room temperature followed by three washes with PHEM/DMSO buffer. Primary antibodies were diluted in 0.5% BSA and hybridized at 37°C for 1 h. Three washes were done with PHEM/DMSO buffer. Secondary antibodies (Jackson Laboratories) conjugated with FITC (fluorescein) or TRITC (rhodamine) were diluted in double-distilled water and hybridized at 37°C for 1 h followed by three washes with double-distilled water. In double-labeling experiments, the antibodies were concomitantly incubated. Primary antibodies were used at the following concentrations: anti-DEK1, 1:300; anti-CR4, 1:300, anti-SAL1, 1:500. Secondary antibodies were used at the following concentrations: anti-rabbit FITC, 1:300; anti-rat TRITC, 1:300; anti-rabbit TRITC, 1:300. The sections were then mounted in Anti-Fade reagent (Molecular Probes), air-dried overnight, and examined by confocal microscopy. To exclude the possibility that DEK1 immunosignals as round structures due to the Triton X-100 treatment in the staining process, we skipped Triton X-100 treatment in immunostaining and found similar DEK1 immunosignals as round structures, indicating that Triton X-100 did not affect the signals (data not shown). Therefore, we routinely treated the specimens with Triton X-100 to permeabilize plasma membranes.

Maize roots were harvested directly from agar plates and fixed in 4% paraformaldehyde in 0.01 M PIPES buffer overnight at 4°C and washed three times for 5 min each in 0.05 M PIPES buffer. Root tips were then cut off and placed on a cover slip with Meyer's adhesive. The root tips were gently crushed between two cover slips to separate the cells. The two cover slips were then covered with a thin film (0.75% low-melting-point agarose and 0.75% gelatin) and washed three times for 5 min each in PHEM buffer. The roots were covered in a freshly prepared enzyme mixture (0.1% cellulose and 0.1% β-glucuronidase) for 1 h to help digest the plant cell wall. The cover slips were washed three times for 5 min each in PHEM buffer before treatment with 1% Triton X-100 to help permeabilize the plasma membrane and then washed again. The cover slips were incubated for 1 h at 37°C in the dark with 1:500 anti-GFP rabbit IgG fraction and Alexa Fluor 594 conjugate (Molecular Probes). The cover slips were washed in the dark three times for 5 min each in PHEM buffer and mounted in ProLong anti-fade mounting medium (Invitrogen). Slides were stored in the dark at 4°C until imaging. Confocal laser scanning microscopy was performed with a Leica SP2 apparatus, and the Alexa Fluor 594 was excited with a He/Ne 568-nm laser.

For immunostaining experiments described in Supplemental Figure 2 online, root tissues from At MEM-DEL-FLAG–expressing 2-week-old *Arabidopsis* plants were harvested. After enzyme treatment with 0.1% cellulose and 0.1% β-glucuronidase for 40 min at room temperature, the cover slips were washed three times for 5 min each with PHEM buffer. The cover slips with root tissue were incubated for 1 h at 37°C in the dark with 1:200 monoclonal anti-FLAGM2-FITC conjugate antibody produced in mouse (Sigma-Aldrich). The cover slips were washed in the dark three times for 5 min each in PHEM buffer and mounted in ProLong anti-fade mounting medium (Invitrogen). Slides were stored in the dark at 4°C until imaging. Confocal laser scanning microscopy was performed with a Leica SP2 apparatus, and the FITC was excited with an argon ion 488-nm laser.

For the immunostaining experiments described in Supplemental Figures 1F and 1G online, in vitro–grown endosperm was harvested directly from agar plates and fixed overnight in 4% paraformaldehyde in 0.1 M PIPES buffer. The tissue was then washed three times for 5 min each in 0.05 M PIPES buffer, infiltrated with TissueTek, and frozen in the cryostat chamber. The chamber was set at −20°C, and the knife was at −21°C. Fourteen-micrometer-thick sections were dried down on precoated glass slides. When the sections had thawed, the slides were washed three times for 5 min each in 0.1 M PBS, then three times for 5 min each with double-distilled water. Autofluorescence was quenched with 0.01% $NaBH_4$ for 2 min at room temperature. The slides were washed three times for 5 min each in water and three times for 5 min each in 0.1 M PBS and blocked with blocker (5% normal donkey serum [Sigma-Aldrich, secondary host], 5% BSA, and 0.01% Triton X-100 in 0.1 M PBS) for 2 h at room temperature. Primary Zm8 antibody was diluted in blocker solution to a working concentration of 1:300 (1×). Peptides were added in 10× excess with the primary antibody, giving three primary antibody solutions: (1) Zm8 (DKGLDPNFSYMLKDK); (2) Zm8 + negative peptide Zm8 (SPNDLKYDFKMDGKL); and (3) Zm8 + original peptide Zm8. The peptides were prediluted to 4 mg/mL in double-distilled water, and the purity was >85% (Genescript).

The antibody–antigene mixture was added to the sections and incubated overnight in a humid chamber at 4°C. Slides were washed three times for 5 min each in 0.1 M PBS. As secondary antibody, Rhodamine Red-X–conjugated AffiniPure donkey anti-rabbit IgG (Jackson ImmunoResearch) was used at a 1:300 dilution with blocking buffer. Secondary antibody was added to the sections and incubated for 30 min at 37°C in the dark. Slides were washed three times for 5 min each in 0.1 M PBS and then three times for 5 min each in double-distilled water before mounting in ProLong anti-fade mounting medium (Invitrogen). Slides were left to dry for 6 h at room temperature and stored in the dark at 4°C until imaging. Confocal laser scanning microscopy was performed with a Leica SP2 confocal microscope. Rhodamine Red was excited with an Ar/Kr 514-nm laser, and FITC was excited with an Ar ion 488-nm laser. Alternatively, we used a Nikon C1 confocal microscope using the EZ C1 program. GFP and FITC were excited by the 488-nm laser line in combination with the main dichroic 545-nm filter and detected by a band-pass 500- to 530-nm filter. TRITC was excited by the 543-nm laser line and detected by a band-pass 570- to 610-nm filter.

Probe-Movement Assays on in Vitro–Grown Endosperms

HPTS (molecular mass of 524 D; Invitrogen) and FITC-conjugated 40-kD dextran (Sigma-Aldrich) were prepared in endosperm liquid culture medium at 5 mg/mL (Kim et al., 2002). Cell walls were stained with a 1 mg/mL solution of Congo Red (Allied Chemical) in the endosperm culture medium. All fluorescent probes were prepared just before the movement assay. In vitro–grown endosperms harvested at 6 DAP and grown in culture for 2 or 5 d were used. Thin slices of tissue were removed with a razor blade at both ends of the cultured endosperms to allow penetration of the fluorescent tracers. The endosperms were incubated in tracer solutions for 10 min at room temperature. Fluorescent tracers were then washed out by rinsing the endosperms three times with fresh endosperm culture medium. Then, transverse slices of the cultured endosperm were stained with the Congo Red solution and visualized using a Zeiss LSM510 Meta microscope using the 488-nm excitation line/505- to 530-nm band-pass filter for FITC detection and the 543-nm excitation line/585- to 615-nm band-pass filter for Congo Red detection.

Light and Scanning Electron Microscopy

For morphological examinations of *Arabidopsis* using light microscopy and scanning electron microscopy, tissues were prepared as described previously by Lid et al. (2004). For light microscopy, sections were cut at 0.5 to 1.0 μm, stained with Stevenels Blue (del Cerro et al., 1980), and viewed using a Leitz Aristoplan microscope, and images were recorded using a DC300F digital camera (Leica). For scanning electron microscopy, samples were critical-point-dried using a CPD 030 (Bal-Tec) drier, coated with ~500 Å Pt in a SC7640 sputter-coater, and analyzed using an EVO-50 microscope (Zeiss).

Transmission Electron Microscopy and Immunogold Labeling

In vitro–grown maize endosperm and pieces of endosperm tissue from developing maize kernels were high-pressure frozen/freeze-substituted for electron microscopy analysis as described by Otegui et al. (2001). For immunogold labeling, some high-pressure-frozen samples were substituted in 0.2% uranyl acetate (Electron Microscopy Sciences) plus 0.2% glutaraldehyde (Electron Microscopy Sciences) in acetone at −80°C for 72 h and then warmed to −50°C for 24 h. After several acetone rinses, these samples were infiltrated with Lowicryl HM20 (Electron Microscopy Sciences) during 72 h and polymerized at −50°C under UV light for 48 h. Sections were mounted on Formvar-coated nickel grids and blocked for 20 min with a 5% (w/v) solution of nonfat milk in PBS containing 0.1% Tween 20. The sections were incubated in the primary antibodies (1:10 in PBS–Tween 20) for 1 h, rinsed in PBS containing 0.5% Tween 20, and then transferred to the secondary antibody (anti-rabbit IgG, 1:50) conjugated to 15-nm gold particles for 1 h. Controls either omitted the primary antibodies or used the preimmune serum.

Electron Tomography

Epon sections (250 nm thick) were mounted on Formvar-coated copper slot grids and stained with 2% uranyl acetate in 70% methanol and Reynold's lead citrate (2.6% lead nitrate and 3.5% sodium citrate, pH 12). Colloidal gold particles (15 nm) were used as fiducial markers for aligning the series of tilted images. The sections were mounted in a tilt-rotate specimen holder and observed in a Tecnai TF30 300-kV intermediate voltage electron microscope (FEI Company) operated at 300 kV. The images were taken at 15,000× from +60°C to −60°C at 1.0°C intervals about two orthogonal axes and collected with a Gatan digital camera at a pixel size of 1.0 nm. The images were aligned as described (Ladinsky et al., 1999). Tomograms were computed for each set of aligned tilts using the R-weighted back-projection algorithm. Merging of the two single-axis tomograms into a dual-axis tomogram involved a warping procedure. Serial tomograms were obtained by combining dual-axis tomograms (Ladinsky et al., 1999). Tomograms were displayed and analyzed with 3Dmod, the graphical component of the IMOD software package (Kremer and Larson, 1983).

Accession Numbers

Sequences of the proteins mentioned in this article can be found in GenBank: human CHMP1 (Q9HD42), *Arabidopsis* DEK1 (NM_104411), loblolly pine DEK1 (AW043258), maize DEK1 (AY061804), yeast class E protein of the vacuolar protein-sorting pathway (DID2) (NP_012961), *Arabidopsis* CR4 (AB074762), maize CR4 (U67422), *Arabidopsis* SAL1 (*Arabidopsis* developmental protein; At1g73030), and maize SAL1 (AY243475). The DEK1 *P. patens* sequence (protein identifier 192068) can be found at http://genome.jgi-psf.org//Phypa1_1/Phypa1_1.home.html.

Supplemental Data

The following materials are available in the online version of this article.

Supplemental Figure 1. Immunostaining of DEK1.

Supplemental Figure 2. Detection of At DEK1-MEM and At DEK1-MEM-DEL in *Arabidopsis*.

Supplemental Figure 3. CR4 Peptide Antibodies Recognized the CR4:HA:FLAG:AcGFP Fusion Protein in Sections of in Vitro Endosperm.

Supplemental Figure 4. DEK1, SAL1, and CR4 Localization in *sal1-2* Mutant Endosperms.

Supplemental Figure 5. Colocalization of CR4 and SAL1 Proteins.

ACKNOWLEDGMENTS

Guru Rao and Suman Kundu are gratefully acknowledged for providing the CR4 antibodies, and Bo Shen and Changjiang Li are acknowledged for providing the SAL1 antibodies. Kimberly Glassman and Shane Abbitt are thankfully acknowledged for the maize vector constructs, and Jerry Ranch is acknowledged for maize transformation work. Hena Guo, Karin S. Olsen, and John Elwer are gratefully acknowledged for help with plant materials, including dissections and maize endosperm in vitro cultures. Paul Anderson is thankfully acknowledged for continued support. We also thank members of the Boulder Laboratory for 3-Dimensional Electron Microscopy of Cells for their support with the electron tomographic analysis. Ragnhild Nestestog at the Norwegian Arabidopsis Research Center is gratefully acknowledged for help with *Arabidopsis* transformation. The confocal imaging of *Arabidopsis* in Supplemental Figures 1F, 1G, 2A, and 2B online was performed at the Molecular Imaging Center (Norwegian Research Council), University of Bergen. Ralph Quatrano is acknowledged for making the *P. patens* DEK1 sequence available prior to publication. This work was supported in part by Norwegian Research Council Grant 159031/I20 and Grant MCB-0619736 from the U.S. National Science Foundation to M.S.O.

Received November 12, 2006; revised September 18, 2007; accepted September 25, 2007; published October 12, 2007.

REFERENCES

Aggarwal, B.B. (2003). Signalling pathways of the TNF superfamily: A double-edged sword. Nat. Rev. Immunol. **3:** 745–756.

Babst, M. (2005). A protein's final ESCRT. Traffic **6:** 2–9.

Becraft, P.W., and Asuncion-Crabb, Y. (2000). Positional cues specify and maintain aleurone cell fate in maize endosperm development. Development **127:** 4039–4048.

Becraft, P.W., Kang, S.-H., and Suh, S.-G. (2001). The maize CRINKLY4 receptor kinase controls a cell-autonomous differentiation response. Plant Physiol. **127:** 486–496.

Becraft, P.W., Li, K., Dey, N., and Asuncion-Crabb, Y. (2002). The maize *Dek1* gene functions in embryonic pattern formation and cell fate specification. Development **129:** 5217–5225.

Becraft, P.W., Stinard, P.S., and McCarty, D. (1996). CRINKLY4: A TNFR-like receptor kinase involved in maize epidermal differentiation. Science **273:** 1406–1409.

Cao, X., Li, K., Suh, S.G., Guo, T., and Becraft, P.W. (2005). Molecular analysis of the *Crinkly4* gene family in *Arabidopsis thaliana.* Planta **220:** 645–657.

Clough, S.J., and Bent, A.F. (1998). Floral dip: A simplified method for *Agrobacterium*-mediated transformation of *Arabidopsis thaliana.* Plant J. **16:** 735–743.

Deblaere, R., Bytebier, B., De Greve, H., Deboeck, F., Schell, J., Van Montagu, M., and Leemans, J. (1985). Efficient octopine Ti plasmid-derived vectors for *Agrobacterium*-mediated gene transfer to plants. Nucleic Acids Res. **13:** 4777–4788.

del Cerro, M., Cogen, J., and del Cerro, C. (1980). Stevenel's Blue, an excellent stain for optical microscopical study of plastic embedded tissues. Microsc. Acta **83:** 117–121.

Dourdin, N., Bhatt, A.K., Dutt, P., Greer, P.A., Arthur, J.S.C., Elce, J.S., and Huttenlocher, A. (2001). Reduced cell migration and disruption of the actin cytoskeleton in calpain-deficient embryonic fibroblasts. J. Biol. Chem. **276:** 48382–48388.

Dutt, P., Croall, D.E., Arthur, S.C., De Veyra, T., Williams, K., Elce, J.S., and Greer, P.A. (2006). m-Calpain is required for preimplantation embryonic development in mice. BMC Dev. Biol. **6:** 3.

Fox, J.E.B., and Saido, T.C. (1999). Calpain in signal transduction. In Calpain: Pharmacology and Toxicology of Calcium-Dependent Protease, K. Wang, ed (Philadelphia: Taylor & Francis), pp. 103–126.

Franco, S., Perrin, B., and Huttenlocher, A. (2004). Isoform specific function of calpain 2 in regulating membrane protrusion. Exp. Cell Res. **299:** 179–187.

Gifford, M.L., Dean, S., and Ingram, G.C. (2003). The *Arabidopsis Acr4* gene plays a role in cell layer organisation during ovule integument and sepal margin development. Development **130:** 4249–4258.

Gifford, M.L., Robertson, F.C., Soares, D.C., and Ingram, G.C. (2005). *Arabidopsis* CRINKLY4 function, internalization and turnover are dependent on the extracellular crinkly repeat domain. Plant Cell **17:** 1154–1166.

Glading, A., Bodnar, R.J., Reynolds, I.J., Shiraha, H., Satish, L., Potter, D.A., Blair, H.C., and Wells, A. (2004). Epidermal growth factor activates m-calpain (calpain II), at least in part, by extracellular signal-regulated kinase-mediated phosphorylation. Mol. Cell. Biol. **24:** 2499–2512.

Goll, D.E., Thompson, V.F., Li, H.R., Wei, W., and Cong, J. (2003). The calpain system. Physiol. Rev. **83:** 731–801.

Gruis, D., Guo, H., Selinger, D.A., Tian, Q., and Olsen, O.-A. (2006). Surface position, and not signaling from surrounding maternal tissues, specify aleurone epidermal cell fate in maize endosperm organ cultures. Plant Physiol. **141:** 898–909.

Howard, T.L., Stauffer, D.R., Degnin, C.R., and Hollenberg, S.M. (2001). CHMP1 functions as a member of a newly defined family of vesicle trafficking proteins. J. Cell Sci. **114:** 2395–2404.

Johnson, K.L., Degnan, K.A., Ross Walker, J., and Ingram, G.C. (2005). *AtDEK* is essential for specification of embryonic epidermal cell fate. Plant J. **44:** 114–127.

Katzmann, D.J., Odorizzi, G., and Emr, S.D. (2002). Receptor down-regulation and multivesicular-body sorting. Nat. Rev. Mol. Cell Biol. **12:** 893–905.

Kidner, C., Sundaresan, V., Roberts, K., and Dolan, L. (2000). Clonal analysis of the *Arabidopsis* root confirms that position, not lineage, determines cell fate. Planta **221:** 191–199.

Kim, I.G., Hempel, F.D., Sha, K., Pfluger, J., and Zambryski, P.C. (2002). Identification of a developmental transition in plasmodesmatal function during embryogenesis in *Arabidopsis thaliana.* Development **129:** 1261–1272.

Kim, Y.-S., Kim, S.-G., Park, J.-E., Park, H.-Y., Lim, M.-H., Chua, N.-H., and Park, C.-M. (2006). A membrane-bound NAC transcription factor regulates cell division in *Arabidopsis.* Plant Cell **18:** 3132–3144.

Kremer, A., and Larson, P.R. (1983). Genetic control of height growth components in jack pine (*Pinus banksiana*) seedlings. Forest Sci. **29:** 451–464.

Ladinsky, M.S., Mastronarde, D.N., McIntosh, J.R., Howell, K.E., and Staehelin, L.A. (1999). Golgi structure in three dimensions: Functional insights from the normal rat kidney cell. J. Cell Biol. **144:** 1135–1149.

Laux, T., Wurschum, T., and Breuninger, H. (2004). Genetic regulation of embryonic pattern formation. Plant Cell **16** (suppl.): S190–S202.

Lee, J.-Y., Taoka, K.-i., Yoo, B.-C., Ben-Nissan, G., Kim, D.-J., and Lucas, W.J. (2005). Plasmodesmal-associated protein kinase in tobacco and *Arabidopsis* recognizes a subset of non-cell-autonomous proteins. Plant Cell **17:** 2817–2831.

Lid, S.E., Al, R.H., Krekling, T., Meeley, R.B., Ranch, J., Opsahl-Ferstad, H.-G., and Olsen, O.-A. (2004). The maize *disorganized aleurone layer 1* and *2* (*dil1, dil2*) mutants lack control of the mitotic division plane in the aleurone layer of developing endosperm. Planta **218:** 370–378.

Lid, S.E., Gruis, D., Jung, R., Lorentzen, J.A., Ananiev, E., Chamberlin, M., Niu, X., Meeley, R., Nichols, S.E., and Olsen, O.-A. (2002). The *defective kernel 1* (*dek1*) gene required for aleurone cell development in the endosperm of maize grains encodes a membrane protein of the calpain gene superfamily. Proc. Natl. Acad. Sci. USA **99:** 5460–5465.

Lid, S.E., Olsen, L., Nestestog, R., Aukerman, M., Brown, R.C., Lemmon, B.E., Mucha, M., Opsahl-Sorteberg, H.-G., and Olsen, O.-A. (2005). Mutation in the *Arabidopsis thaliana Dek1* calpain gene perturbs endosperm and embryo development while over-expression affects organ development globally. Planta **221:** 339–351.

Locksley, R.M., Killeen, N., and Lenardo, M.J. (2001). The TNF and TNF receptor superfamilies: Integrating mammalian biology. Cell **104:** 487–501.

MacEwan, D.J. (2002). TNF receptor subtype signalling: Differences and cellular consequences. Cell. Signal. **14:** 477–492.

Mellman, I. (1996). Endocytosis and molecular sorting. Annu. Rev. Cell Dev. Biol. **12:** 575–625.

Murashige, T., and Skoog, T. (1962). A revised medium for rapid growth and bioassays with tobacco tissue culture. Physiol. Plant. **15:** 473–497.

Nickerson, D.P., West, M.A., and Odorizzi, G. (2006). Did2 coordinates Vps4-mediated dissociation of ESCRT-III from endosomes. J. Cell Biol. **175:** 715–720.

Otegui, M.S., Mastronarde, D.N., Kang, B.-H., Bednarek, S.Y., and Staehelin, L.A. (2001). Three-dimensional analysis of syncytial-type cell plates during endosperm cellularization visualized by high resolution electron tomography. Plant Cell **13:** 2033–2051.

Quatrano, R.S., McDaniel, S.F., Khandelwal, A., Perroud, P.F., and Cove, D.J. (2007). *Physcomitrella patens*: Mosses enter the genomic age. Curr. Opin. Plant Biol. **10:** 182–189.

Russell, D.A., and Fromm, M.E. (1997). Tissue-specific expression in transgenic maize of four endosperm promoters from maize and rice. Transgenic Res. **6:** 157–168.

Saito, K., Elce, J.S., Hamos, J.E., and Nixon, R.A. (1993). Widespread activation of calcium-activated neutral proteinase (calpain) in the brain

in Alzheimer disease: A potential molecular basis for neuronal degeneration. Proc. Natl. Acad. Sci. USA **90:** 2628–2632.

Savaldi-Goldstein, S., Peto, C., and Chory, A. (2007). The epidermis both drives and restricts plant shoot growth. Nature **446:** 199–202.

Shen, B., Li, C., Min, Z., Meeley, R.B., Tarczynski, M.C., and Olsen, O.-A. (2003). sal1 determines the number of aleurone cell layers in maize endosperm and encodes a class E vacuolar sorting protein. Proc. Natl. Acad. Sci. USA **100:** 6552–6557.

Stewart, R.N., and Dermen, H. (1975). Flexibility in ontogeny as shown by the contribution of the shoot apical layers to the leaves of periclinal chimaeras. Am. J. Bot. **62:** 935–947.

Takada, S., and Jürgens, G. (2007). Transcriptional regulation of epidermal cell fate in the *Arabidopsis* embryo. Development **134:** 1141–1150.

Tanaka, H., Watanabe, M., Watanabe, D., Tanaka, T., Machida, C., and Machida, Y. (2002). *ACR4*, a putative receptor kinase gene of *Arabidopsis thaliana*, that is expressed in the outer cell layers of embryos and plants, is involved in proper embryogenesis. Plant Cell Physiol. **43:** 419–428.

Ueda, T., and Messing, J. (1991). A homologous expression system for cloned zein genes. Theor. Appl. Genet. **82:** 93–100.

Wang, C., Barry, J.K., Min, Z., Tordsen, G., Rao, A.G., and Olsen, O.-A. (2003). The calpain domain of the maize DEK1 protein contains the conserved catalytic triad and functions as a cysteine proteinase. J. Biol. Chem. **278:** 34467–34474.

Watanabe, M., Tanaka, H., Watanabe, D., Machida, C., and Machida, Y. (2004). The ACR4 receptor-like kinase is required for surface formation of epidermis-related tissues in *Arabidopsis thaliana.* Plant J. **39:** 298–308.

Xu, Y.H., and Mellgren, R.L. (2002). Calpain inhibition decreases the growth rate of mammalian cell colonies. J. Biol. Chem. **277:** 21474–21479.

Yang, K.S., Jin, U.H., Kim, J., Song, K., Kim, S.J., Hwang, I., Lim, Y.P., and Pai, H.S. (2004). Molecular characterization of NbCHMP1 encoding a homolog of human CHMP1 in *Nicotiana benthamiana.* Mol. Cells **17:** 255–261.

Yu, T., Wu, C., De Veyra, T., and Greer, P.A. (2006). Ubiquitous calpains promote both apoptosis and survival signals in response to different cell death stimuli. J. Biol. Chem. **281:** 17689–17698.

Zalewska, T., Thompson, V.F., and Goll, D.E. (2004). Effect of phosphatidylinositol and inside-out erythrocyte vesicles on autolysis of mu- and m-calpain from bovine skeletal muscle. Biochim. Biophys. Acta **1693:** 125–133.

Zhao, Z.Y., and Ranch, J. (2006). Transformation of maize *via Agrobacterium tumefaciens* using a binary co-integrate vector system. Methods Mol. Biol. **318:** 315–323.